Alterations in oxidative responses and post-translational modification caused by *p,p´*-DDE in *Mus spretus* testes reveal Cys oxidation status in proteins related to cell-redox homeostasis and male fertility

José Alhama[1], Carlos A. Fuentes-Almagro[2], Nieves Abril[1], Carmen Michán[1,*]

[1]Departamento de Bioquímica y Biología Molecular, Campus de Excelencia Internacional Agroalimentario CeiA3, Universidad de Córdoba, Campus de Rabanales, Edificio Severo Ochoa, E-14071, Córdoba, España, Spain

[2]Servicio Central de Apoyo a la Investigación (SCAI), Unidad de Proteómica, Universidad de Córdoba, Campus de Rabanales, Edificio Ramón y Cajal, E-14071, Córdoba, España, Spain

*Corresponding author. Department of Biochemistry and Molecular Biology, Building Severo Ochoa, 2nd floor, Campus de Rabanales, University of Córdoba, 14071, Córdoba, Spain. Tel.: + 34 957 218082.

E-mail address: bb2midoc@uco.es (C. Michán).

Keywords:

Organochlorine pesticides; Mice testes; Oxidative stress; Label-based redox proteomic; Post-translational modifications; Reproduction.

ABSTRACT

The major derivate of DDT, 1,1-dichloro-2,2-bis (p-chlorophenyl) ethylene (*p,p´*-DDE), is a persistent pollutant previously associated with oxidative stress. Additionally, *p,p´*-DDE has been linked to several metabolic alterations related to sexual function in rodents. In this study, we analysed the effects of a non-lethal *p,p´*-DDE dose to *Mus spretus* mice in testes, focusing on oxidative damage to biomolecules, defence mechanisms against oxidative stress and post-translational protein modifications. No increase in lipid or DNA oxidation was observed, although antioxidative enzymatic defences and redox status of glutathione were altered in several ways. Global protein carbonylation and phosphorylation were significantly reduced in testes from *p,p´*-DDE-exposed mice; however, the total redox state of Cys thiols did not exhibit a defined pattern. We analysed the reversible redox state of specific Cys residues in detail with differential isotopic labelling and a shotgun labelling-based MS/MS proteomic approach for identification and quantification of altered peptides. Our results show that Cys residues are significantly affected by *p,p´*-DDE in several proteins related to oxidative stress and/or male fertility, particularly those participating in fertilization, sperm capacitation and blood coagulation. These molecular changes could explain the sexual abnormalities previously described in *p,p´*-DDE exposed organisms.

1. Introduction

A large variety of synthetic organic chemicals, such as organochlorine pesticides (OCPs), have been released into the environment over the last few decades (Valeron et al., 2009). As widespread environmental pollutants, OCPs are highly lipophilic and chemically stable compounds that persist in the environment and accumulate in both the food chain and human tissues (Alvarez-Pedrerol et al., 2008); 2,2-bis (4-chlorophenyl)-1,1,1-trichloroethane (*p,p´*-DDT), the first widely used synthetic organochlorine pesticide, was given credit for having helped one billion people live malaria-free. Although banned for agricultural use in the 1970s-1980s, several kilotons had already been released into the environment (Stemmler and Lammel, 2009), and *p,p´*-DDT's bioaccumulation, long-range transport, persistence in the environment, and anti-androgenic properties have caused concern about its ecological effects. Furthermore, although having being banned or restricted for three decades, *p,p´*-DDT is still being used for the control of vectors in public health in some developing (Aulakh et al., 2007; Lopez-Carrillo et al., 1996; Rivero-Rodriguez et al., 1997; Zhang et al., 2013).

1,1-dichloro-2,2-bis (p-chlorophenyl) ethylene (*p,p´*-DDE) is DDT's major metabolite and, as such, is the form most commonly found in human tissues at the highest concentration (Rogan and Chen, 2005). In 2002, it was reported that this pollutant was present in the sera of more than 90% of the population of North America (Daxenberger, 2002). Recently, high levels of DDT metabolites, including *p,p´*-DDE, have been detected in human milk samples, particularly from less industrialized countries (van den Berg et al., 2017). Moreover, new determinations of these pollutants in China show that their levels have not significantly declined over time, and

63 are reaching very toxic concentrations in harbour environments, both in biotic and
64 abiotic samples, where dietary seafood intake can cause deleterious effects in human
65 health (Zhang et al., 2013). Additionally, *p,p´*-DDE has been reported to be a
66 widespread environmental endocrine disrupting chemical, associated with
67 abnormalities in sexual development in rats and wildlife (Gray and Kelce, 1996; Kelce
68 et al., 1995). Moreover, *p,p'*-DDE is anti-androgenic and can inhibit androgen binding
69 to the androgen receptor (Kelce et al., 1995; Xu et al., 2006), and high *p,p'*-DDE-DDT
70 levels significantly increase the risk for low sperm count (Messaros et al., 2009).
71 Despite the molecular mechanisms for *p,p´*-DDE adverse androgenic effect
72 being incompletely understood, ROS generation has been suggested to play a critical
73 role in disrupting testis function (Shi et al., 2009; Song et al., 2008). Certain pesticides
74 induce oxidative stress through generation of ROS, highly toxic and mutagenic species,
75 mediating damage to biomolecules and altering the content and redox status of
76 glutathione (Sies, 1986). To protect from oxidative stress, aerobic organisms use
77 several lines of defence. Primary antioxidant enzymes, such as catalase (CAT), detoxify
78 ROS, while others act as ancillary antioxidant enzymes, such as glutathione reductase
79 (GSR), which uses NADPH to turn oxidized glutathione (GSSG) into its reduced form
80 (GSH). Glutathione is an abundant thiol that keeps the cytosol reduced and is related
81 to a third line of defence that cooperates with enzymatic defences (Sies, 1986). Both
82 damage to biomolecules and antioxidative defence mechanisms are highly sensitive to
83 pollutants that generate oxidative stress (López-Barea, 1995).
84 ROS are considered important second messengers since they mediate redox-
85 signalling cascades that are critical to numerous physiological and pathological
86 processes. As a consequence of ROS exposure, a range of reversible and irreversible

post-translational modifications (PTMs) have been described that play essential roles in cellular localization, protein-protein interactions, protein structure and biological activity (Cabiscol and Ros, 2006; Davies, 2005; Eaton, 2006; Levine, 2002; Sheehan et al., 2010). Redox proteomics aim to detect and analyse redox-based changes within the proteome both in redox signalling scenarios and during oxidative stress (Sheehan et al., 2010). Formation of non-reversible carbonyl groups (Chaudhuri et al., 2006; Yan and Forster, 2011) and reversible modification of redox-sensitive thiol groups on cysteine (Cys) residues (Fernandez-Cisnal et al., 2014; Sheehan et al., 2010; Ying et al., 2007) are major forms of protein oxidation that are widely used indicators of oxidative stress. Unlike irreversible oxidative damage, redox signalling operates as a reversible "redox switch" that allows rapid responses to physiological and environmental cues (Morales-Prieto and Abril, 2017; Sheehan et al., 2010; Ying et al., 2007). Phosphorylation/dephosphorylation of proteins is another common PTM that is an important modulator of protein function, thus playing a major role in the regulation of various bio-signalling pathways (Graves and Krebs, 1999; White, 2008). Gel electrophoresis-based redox proteomics approaches are commonly used to evaluate protein oxidation/modification levels. Several chemical probes have been used for specific detection and quantification of different PTMs. Among these, fluorescence labelling offers advantages when used in gel-based analysis for the following reasons: i) it provides high sensitivity with short analysis times; ii) unbound probes are separated from proteins during gel electrophoresis; and iii) the same gel can be used for both specific PTM staining and total protein imaging (Yan and Forster, 2011).

Redox signalling has been proposed as the central mechanism underlying toxicological effects of many environmental toxicants, including pesticides such as *p,p´*-

111 DDE (Morales-Prieto and Abril, 2017). Although cysteine residues are scarce in
112 proteins, representing only 1-3% of total protein residues, they are one of the most
113 reactive residues. The electronegativity of sulphur atoms in the thiolate group of
114 cysteine side chain renders Cys vulnerable to many electrophiles, such as ROS, leading
115 to redox modification (Eaton, 2006; Sheehan et al., 2010; Winterbourn and Hampton,
116 2008; Ying et al., 2007). Redox proteomics refers to different methods used for the
117 detection, quantification and identification of oxidant-sensitive thiol proteins (Eaton,
118 2006; Sheehan et al., 2010). However, the current trend is to use gel-free proteomics
119 techniques, which are less time-consuming and labour-intensive than 2DE and allow
120 for higher sample throughput (Sheehan et al., 2010). A novel redox proteomic
121 approach uses liquid chromatography-tandem mass spectrometry (LC-MS/MS analysis)
122 to identify and quantify the reversible redox state of specific Cys residues after
123 differential labelling of reversibly oxidized and reduced Cys residues in peptides with
124 light (d0) and heavy (d5) forms of the thiol alkylating reagent *N*-ethylmaleimide (NEM)
125 (McDonagh et al., 2014).

126 *Mus musculus* mouse strains commonly used for laboratory analysis are
127 artificial hybrids that present few natural genetic polymorphisms (Dejager et al., 2009).
128 In contrast, *Mus spretus* strains are only moderately inbred and therefore have a larger
129 reservoir for phenotypic variation. Additionally, these mice belong to an unprotected
130 species broadly found in Southern Spain and Northern Africa. These qualities make *M.*
131 *spretus* rodents valuable bioindicators for studying complex effects (Dejager et al.,
132 2009; Dejager et al., 2010); as such, they have been utilized in several laboratories,
133 including our own, for environmental monitoring and in-lab exposure experiments
134 (Abril et al., 2015; Garcia-Sevillano et al., 2014; Morales-Prieto and Abril, 2017).

As described above, *p,p´*-DDE is a hormone disruptor that alters male fertility in humans and other animals, affecting semen quality (Quan et al., 2016; Song et al., 2014a). Molecularly, DDT/DDE-induced toxicity has been associated with induction of oxidative stress and mitochondrial dysfunction by several groups (Harada et al., 2016; Li et al., 2017; Morales-Prieto and Abril, 2017; Morales-Prieto et al., 2017). Thus, this study was designed to explore the biological effects of *p,p´*-DDE in mice testes, particularly those related to oxidative stress. Specifically, we aimed to determine the molecular effects of a sub-lethal dose of *p,p´*-DDE on mice testes by studying several biochemical parameters related to stress and oxidative response. We investigated antioxidative enzymes, lipid peroxidation, DNA damage, glutathione levels and protein posttranslational modifications (carbonylation, thiol oxidation and phosphorylation). Furthermore, we assessed the redox state of the testis proteome by massive mass spectrometry after differential isotopic labelling of oxidized and reduced Cys-containing peptides.

2. Materials and methods

2.1 Animals and experimental design

This study was performed with all ethical requirements demanded by the Bioethical Committee of the University of Córdoba (Spain). *M. spretus* mice belonging to the inbred lineage SPRET/EiJ were utilized for these experiments. They originate from wild mice caught at Puerto Real (Cádiz, Spain) that were inbred over more than 65 generations in the Jackson Lab (EEUU). During experiments, animals were housed at the Animal Experimentation Service of the University of Córdoba (SAEX-UCO) with controlled light/dark photoperiod (12/12 h) and 25 ± 2°C temperature, plus *ad libitum*

159 food and water. All exposed individuals were eight-week-old consanguineous male
160 mice (11-13 g weight). Experimental animals were randomly divided into two groups of
161 four mice each. The control group was fed Teklad Global 14% Protein Rodent
162 Maintenance diet (Envigo; Ref. 2004; http://www.envigo.com/resources/data-
163 sheets/2014-dataheet-0915.pdf) mixed with 3 ml refined corn oil per 100 mg feed for
164 30 days. The diet of the two exposed groups contained 0.15 mg/g *p,p´*-DDE (SUPELCO
165 Analytical, SIGMA-ALDRICH), resulting in a daily ingestion of 37.5 µg/g body weight
166 after 10 (DDE10) or 30 days (DDE30) treatment. Both water and food were changed
167 every three days to ensure the maintenance of their properties, and the amount of
168 feed removed was weighed to calculate the ingested dose. *p,p´*-DDE did not
169 significantly affect body mass or testis weight (data not shown). No apparent disease
170 signals or changes in behaviour were observed during the experiment.
171 After the exposure, mice were anaesthetized with isoflurane (1.5%) and
172 sacrificed by cervical dislocation. The testes were removed and weighed. A longitudinal
173 section of one testis from each animal was excised and immediately fixed in formalin
174 and later processed for hematoxylin/eosin (H&E) staining. The remaining fragment and
175 the other testis were preserved in liquid nitrogen. When needed, testes were
176 individually processed with a Freezer/Mill® Grinder (SPEX Sample PreP) and kept at -
177 80°C.
178
179 *2.2 Testis extracts preparation*
180 The testes from each mouse (approximately 100 mg) were mixed with 0.5 ml 50
181 mM Tris ClH pH 7.4, 1 mM EDTA, and 1 mM PMSF buffer and individually homogenized
182 inside 2 ml Eppendorf tubes. During processing, samples were kept cold with liquid N_2.

A further 0.5 ml buffer was added after homogenization. Extracts were then aliquoted for three uses: (i) without further manipulation for DNA analysis, (ii) plus several passages through a 26-width (0.4 mm) needle for malondialdehyde determination, or (iii) further centrifuged (16,200 *g*, 15´, 4°C) for protein/enzymatic assays.

2.3 Oxidative damage to biomolecules

Malondialdehyde (MDA) was detected fluorometrically in the homogenates using the thiobarbituric acid (TBA) reactivity assay. Briefly, 15 µl of each lysate were mixed with 125 µl 0.5% (W/v) in methanol) butylated hydroxytoluene (BHT), 50 µl 0.66 N H_2SO_4 and 37.5 µl 0.4 M Na_2WO_4. Final volume was adjusted to 1 ml with milli-Q water. After centrifugation (5,000 g, 5 min at room temperature), 250 µl 1% (w/v in NaOH) TBA were added to the supernatants, and the mixture was placed in hot water (95°C) for 1 h. Once at room temperature, fluorescence was determined at Ex/Em 515/550 nm, 15 nm 230 slit width, using an LS 50B Fluorescence Spectrometer. MDA concentrations were determined according to a standard curve generated by 1,1,3,3-tetramethoxypropane (TMP) and expressed in pmol mg^{-1} protein.

DNA oxidative damage was measured using an ELISA (OxiSelect™ Oxidative DNA Damage ELISA kit, Cell Biolabs, Inc., San Diego, CA, USA) on microtiter plates according to the manufacturer's specifications. The concentration of 8-OHdG was calculated with a calibration line obtained from known amounts and is expressed in ng mg^{-1} DNA.

2.4 Enzymatic antioxidant activities and total glutathione determination

206 Enzymatic activities were assayed spectrophotometrically using a DU®650
207 Spectrophotometer (Beckman Coulter, Brea, CA, USA) according to previously
208 published protocols routinely applied in our group (Bonilla-Valverde et al., 2004;
209 Ghedira et al., 2011; Montes Nieto et al., 2010; Morales-Prieto and Abril, 2017;
210 Rodriguez-Ariza et al., 1992; Rodriguez-Ariza et al., 1993; Ruíz-Laguna et al., 2001).
211 Protocols are briefly described below.
212 Catalase (CAT) activity was determined by the breakdown of hydrogen peroxide
213 measured at 240 nm. The reaction was performed in 17 mM potassium phosphate
214 buffer, pH 7.0 and 20 mM H_2O_2. Specific activity is expressed as µmol H_2O_2 consumed
215 per min (UI) and mg of protein using an extinction coefficient of 0.04 mM^{-1} cm^{-1}.
216 Glutathione reductase (GR) activity was detected by β-NADPH consumption at
217 340 nm in the presence of oxidized glutathione (GSSG). The reaction mixture contained
218 120 mM potassium phosphate buffer, pH 7.2, 0.275 mM EDTA, 2.125 mM GSSG and
219 0.1625 mM β-NADPH. Specific activity is given in nmol β-NADPH consumed per min
220 (mUI) and mg protein using an extinction coefficient of 6.22 mM^{-1} cm^{-1}.
221 Reduced and oxidized glutathione were determined using GSH/GSSG Ratio
222 Detection Assay Kit (Fluorometric - Green) on microtiter plates according to the
223 manufacturer's specifications (Abcam, Cambridge, United Kingdom).
224 Protein concentration was determined by the Bradford method (Bio-Rad
225 Protein Assay) using bovine serum albumin (BSA) as a standard.
226
227 *2.5 Electrophoresis-based evaluation of post-translational modifications*
228 The Pro-Q® Diamond phosphoprotein gel stain (Molecular Probes®, Invitrogen)
229 was used for selectively staining proteins in polyacrylamide gels following the

manufacturer's recommendations. We analysed 25 µg of protein by SDS-polyacrylamide gel electrophoresis on 4% (w/v) stacking gel and 12% separating gel using the Laemmli buffer system. Samples were separated at 200 V constant in a Mini-PROTEAN 3 Cell (Bio-Rad, Hercules, CA, USA). After electrophoresis, manufacturer´s recommendations were followed for specific staining of phosphoproteins in the gel. Briefly, proteins in the gel were fixed first with a methanol:acetic acid (50:10) solution and, after washing with ultrapure water, Pro-Q® Diamond staining was added and maintained for 90 min under gentle agitation. Next, gels were destained with a 20% acetonitrile, 50 mM sodium acetate, pH 4 solution (30 min, 3 times), washed with ultrapure water, and scanned using a ChemiDoc™ MP Imaging System (Bio-Rad) at 555/580 nm excitation/emission detection wavelengths to show phosphorylated proteins. Gels were then stained with SYPRO Ruby (Bio-Rad) and rescanned at 532/555 nm excitation/emission detection to show total protein. Determining the ratio of Pro-Q Diamond dye to SYPRO Ruby dye signal intensities provides a measure of phosphorylation level normalized to total amount of protein. Image Lab software (Bio-Rad) was used for acquisition of gel images and all subsequent image analyses.

Protein carbonyls were quantified by labelling oxidized proteins with fluorescein-5-thiosemicarbazide (FTC) followed by separating of labelled proteins by gel electrophoresis (Chaudhuri et al., 2006). Briefly, the cytosolic extracts were diluted to 1 mg/ml, and then FTC was added to a final concentration of 1 mM followed by incubation at 37°C for 150 min in the dark. Laemmli treatment buffer was then added and 10 µg of proteins were loaded on 12% SDS-PAGE gels and separated in a Mini-PROTEAN® 3 Cell (Bio-Rad), avoiding light. After electrophoresis, the free residual FTC was removed by extensive washing of the gel with ethanol:acetic acid (50:3) and then

images of the fluorescent protein on the gel was captured using the ChemiDoc™ MP Imaging System (Bio-Rad) at 488/520 nm excitation/emission detection wavelength. Gels were then re-stained with Coomassie brilliant blue R-250 (Bio-Rad) and re-scanned to visualize total protein. Determining the ratio of FTC-labelled proteins to Coommassie signal intensities provides a measure of the carbonylation level normalized to the total protein. Image Lab software (Bio-Rad) was used for acquisition of gel images and all subsequent image analyses.

A fluorescence-based electrophoretic assay was used to quantify both the global level of reversibly oxidized thiols and reduced thiols in proteins whose ratio indicated redox status. Cysteinyl protein thiols were directly labelled with 5-Iodoacetamido-fluorescein (IAF) for native reduced groups. For oxidized thiol detection, all free thiol groups were first blocked with iodoacetamide (IAM), reversibly oxidized thiols were next reduced with tributylphospine (TBP), and the reduced thiols generated were labelled with IAF. In short, for reduced thiol groups, 100 µg protein extracts were denatured by incubating for 10 min at 37°C in 50 µl Tris-HCl 0.1 M, pH 7.4, and 1% SDS. IAF was then added to 200 µM final concentration and samples were incubated for 30 min at 37°C in the dark. After adding Laemmli treatment buffer, proteins were loaded on 12% SDS-PAGE gels and separated in a Mini-PROTEAN® 3 Cell (Bio-Rad, Hercules, CA, USA), avoiding light. To minimize background, gels were destained in ethanol:acetic acid (50:3) before scanning for fluorescence using a ChemiDoc™ MP Imaging System (Bio-Rad) at 488/530 nm excitation/emission detection wavelength to show AF-labeled proteins. For normalization, gels were re-stained with Coomassie, and then the image analysis was carried out as indicated in the previous section. For determination of oxidized thiol groups, the initial reduced

groups in 200 µg protein extracts were blocked by incubating for 30 min at 37°C in Tris-HCl 0.1 M, pH 7.4, 1% SDS and 200 mM IAA. To remove excess IAA, proteins were precipitated with cold 20% Trichloroacetic acid (TCA) followed by three washes with ethanol:ethyl acetate (50:50, v:v). The final pellet was resuspended in Tris-HCl 0.1 M, pH 7.4, 1% SDS and 1 mM TBP to reduce oxidized thiols, and the procedure then continued as in the initially reduced thiol groups. Approximately 20 µg of proteins were loaded on the gels for both reduced and oxidized thiols determinations.

2.6 Label-based MS-based evaluation of the redox status of Cys-containing peptides

We followed a protocol for redox proteomic analysis similar to a previous publication (McDonagh et al., 2014). Briefly, protein extracts were prepared using a hand homogenizer in the presence of blocking buffer containing 25 mM d(0)-NEM and 50 mM ammonium bicarbonate, pH 8, under anaerobic conditions. Protein lysates were cleared by centrifugation and protein concentration was estimated by Bradford assay (Bio-Rad). Extracts were desalted using Pierce™ Polyacrylamide Spin Desalting Columns (7K MWCO; Thermo Fisher Scientific, Waltham, MA, USA) with 25 mM ammonium bicarbonate buffer, pH 8, and protein concentrations were recalculated as before. 200 µg of desalted protein samples were diluted up to 160 µl in ammonium bicarbonate buffer and denatured by addition of 10 µl of 1% w/v RapiGest (Waters, Milford, MA, USA) in the same buffer followed by incubation at 80°C for 10 min. Reversibly oxidized Cys residues were reduced by addition of 10 µl 100 mM TCEP and incubated at 60°C for 10 min. Finally, newly reduced Cys residues were alkylated with 10 µl of 200 mM d(5)-NEM with further incubation for 30 min at room temperature.

To identify proteins containing labelled Cys residues, samples were tryptic digested and analysed by LC-MS/MS at the Proteomic Facility of the University of Córdoba (SCAI, Proteomic Unit). Briefly, 1 µg peptides were separated in Nano-LC Dionex Ultimate 3000 nano UPLC (Thermo Fisher Scientific) with a C18 75 µm x 50 Acclaim Pepmam column (Thermo Fisher Scientific). The peptide mix was previously loaded on a 300 µm x 5 mm Acclaim Pepmap precolumn (Thermo Fisher Scientific) in 2% acetonitrile/0.05% TFA for 5 min at 5 µl/min. Peptide separation was performed at 40°C for all runs. Mobile phase buffer A was composed 0.1% formic acid in water. Mobile phase B was composed of 80% acetonitrile, 0.1% formic acid. Samples were separated at 300 nl/min. Elution conditions were as follows: 4-35% B for 60 min; 35-55% B for 4 min; 55-90% B for 3 min followed by 8 min wash at 90% B and a 10-min re-equilibration at 4% B. Total time for chromatography was 85 min.

Eluted peptide cations were converted to gas-phase ions with nano electrospray ionization and analysed on a Thermo Orbitrap Fusion (Q-OT-qIT; Thermo Fisher Scientific) mass spectrometer operated in positive Data Dependent Acquisition (DDA) mode. Data Survey scans of peptide precursors from 400 to 1500 m/z were performed at 120K resolution (at 200 m/z) with a 4×10^5 ion count target. Tandem MS was performed by isolation at 1.2 Da with the quadrupole, Collision-Induced Dissociation (CID) fragmentation with normalized collision energy of 35, and rapid scan MS analysis in the ion trap. The Automatic Gain Control (AGC) ion count target was set to 2×10^3 and the max injection time was 300 ms. Only those precursors with charge state 2–5 were sampled for MS2. The dynamic exclusion duration was set to 15 s with a 10-ppm tolerance around the selected precursor and its isotopes. Monoisotopic precursor selection was turned on. The instrument was run in top 30 mode with 3 s

cycles, meaning the instrument would continuously perform MS2 events until a maximum of top 30 non-excluded precursors or 3 s, whichever is shorter.

Raw data were processed using Proteome Discoverer (version 2.1.0.81, Thermo Fisher Scientific). MS2 spectra were searched using the SEQUEST engine against a database of Uniprot_Mus musculus_Feb2017 (www.uniprot.org). Peptides were generated by theoretical tryptic digestion, allowing up to one missed cleavage; d(5)-NEM, NEM of cysteines and oxidation of methionine were set as variable modification. Precursor mass tolerance was 10 ppm and product ions were searched at a 0.1 Da tolerance. Peptide Spectral Matches (PSM) were validated using percolator based on q-values at a 1% False Discovery Rate (FDR). Peptide identifications were grouped into proteins with Proteome Discoverer 2.1 according to the law of parsimony and filtered to 1% FDR.

Analysis of identified peptides was performed using Skyline software (http://proteome.gs.washington.edu/software/skyline) in MS1 filtering mode, as was previously described (Schilling et al., 2012). Briefly, comprehensive spectral libraries were first generated in Skyline from database searches in Proteome Discoverer 2.1 of the raw data files prior to MS1 filtering. Second, all raw files acquired in DDA were directly imported into Skyline, and MS1 precursor ions were extracted for all peptides present in the MS/MS spectral libraries. Quantitative MS1 analysis was based on extracted ion chromatograms (XICs) and for the top three resulting precursor ion peak areas *e.g.* M, M+1, and M+2. The ratio between oxidized/reduced Cys peptides was calculated from the total peak areas of precursor ions.

A Cytoscape plug-in, ClueGo, was used for biological interpretation of identified proteins containing differentially oxidized cysteines (Bindea et al., 2009).

2.7 Label Free Quantification

Label Free Quantification (LFQ) intensities were used to determine global levels of the proteins containing peptides with differentially oxidized Cys residues. Raw data were processed using MaxQuant software (version 1.5.5.1) (Cox and Mann, 2008). MS2 spectra were searched with Andromeda engine against the same database used in 2.6 section. Peptides were generated by theoretical tryptic digestion allowing up to one missed cleavage, NEM and d(5)NEM as variable modifications in Cys, and also oxidation as variable modification of methionine. Precursor mass tolerance was 10 ppm and product ions were searched at 0.1 Da tolerance. To validate Peptide Spectral Matches (PSM) in MaxQuant, a target-decoy search strategy was applied. Protein quantification were carried out with MaxLFQ label-free quantification method (Cox et al., 2014), applying retention time alignment and identification transfer protocol ("match-between-runs" feature in MaxQuant).

Differentially expressed proteins analysis was performed with the freely available software Perseus (version 1.5.6.0) (http://www.coxdocs.org/doku.php?id=perseus:start). The peak intensities across the whole set of quantitative data for all of the peptides in the samples were imported from the MaxQuant analysis. Protein quantification data were transformed to logarithmic scale with base 2, and their identities filtered at least in two replicates per condition.

2.8 Statistics

Statistical significance was evaluated using ANOVA, followed by post hoc multiple comparison according to Dunnet for parametric analysis or Kruskal-Wallis for non-parametrix ones, using InStat software. Statistically significant differences are expressed as **, $p < 0.01$; *, $p < 0.05$.

3. Results and Discussion

The experimental procedure did not cause lethality nor deceptive alterations in global mice health. The dissection of the animals did not indicate any visible alteration of the internal organs. No differences in aspect or weight were observed between the testes coming from control or treated mice after the different treatment times (data not shown).

3.1 Histopathological effect of p,p´-DDE in mouse testis

The histological analysis indicated that the treatment did not altered the normal structure of the seminiferous tubules (ST), neither the apparent capability of sperm production, though a slight enlargement of ST size of was observed after the 30 days treatment (Fig. 1). Although *p,p´*-DDE has been associated with sperm malformation, and density and motility alterations (Quan et al., 2016), our results show no variation in testis tissue, and agree with the fact that in humans at low exposure levels no changes in sperm concentration or morphology have been detected (Toft, 2014).

3.2 Oxidative effect of p,p´-DDE to biomolecules in mouse testis

p,p´-DDE exposure has been previously linked to ROS production in rodent testes and human colorectal cells, both indirectly *in vivo* and directly *in vitro* (Shi et al., 2010; Song et al., 2014a; Song et al., 2008; Song et al., 2011; Song et al., 2014b). ROS are extremely harmful to organisms because they can damage biomolecules, such as lipids, proteins and DNA, and they can alter the levels of glutathione and its redox state (Sies, 1986). Fig. 2 shows the levels of different biomarkers of oxidative damage in the testes of mice exposed to *p,p´*-DDE. Lipids are particularly susceptible to oxidation due to their long-hydrogenated chains that are susceptible to peroxidation, which alters membranes and significantly affects cellular functioning. Additionally, lipid-derived radicals can also function as ROS that subsequently damage other biomolecules. MDA was selected as the biomarker for lipid damage because it is the principal and most studied by-product of polyunsaturated fatty acid peroxidation (Brown and Kelly, 1996; Gutteridge, 1984). Fig. 2A shows MDA levels in testis from *p,p´*-DDE-exposed mice and controls, both of individual animals and grouped by treatment. Testes from control mice noticeably showed high levels of individual variability in MDA levels, varying from to 22 to 60 pmol mg^{-1} cell-free extract. In contrast, *p,p´*-DDE intake, during both 10 and 30 days exposure time, provoked a decrease in the variability of MDA content among individuals, as levels measured after both treatments (DDE10 and DDE30) were narrowly distributed between 27 and 38 pmol mg^{-1}. Although no significant changes linked to *p,p´*-DDE intake were observed, global variations suggest that *p,p´*-DDE intake in these conditions somewhat reduced lipid peroxidation in the testis, but variability in controls prevented us from drawing conclusive results. Previous reports obtained with rats exposed to similar *p,p´*-DDE doses demonstrate mixed results, as *p,p´*-DDE is associated with an increase in MDA

levels in testis (Shi et al., 2010), but the same authors later described a non-significant reduction in serum peroxidation after *p,p´*-DDE exposure (Shi et al., 2011).

To evaluate DNA damage induced by *p,p´*-DDE, we measured 8-OHdG levels (Fig. 2B). There were no obvious differences in 8-OHdG levels that could be linked to *p,p´*-DDE, suggesting that this compound does not cause this type of DNA damage in *M. spretus* testis at the doses and times measured. Similar to lipid peroxidation measurements, differences observed among individual animals were once again more evident in controls than in treated groups. The lack of oxidative DNA damage related to *p,p´*-DDE is in agreement with previous reports on this pollutant's effect in human lymphocytes (Geric et al., 2012), although it has been associated with an increase in other DNA lesions, such as double strand DNA breaks in exposed children (Perez-Maldonado et al., 2006).

3.3 Effect of p,p´-DDE on antioxidative defence mechanisms in mouse testes

To assess antioxidative/protective response to *p,p´*-DDE in testis, the activity of two of the main antioxidant enzymes, catalase (CAT) and glutathione reductase (GSR), was determined (Fig. 3). As illustrated in Fig. 3A, administration of *p,p´*-DDE for 10 days significantly diminished catalase activity in mouse testes, a result that was maintained after 30 days exposure (61 and 57% relative to control mice, respectively). In contrast, *p,p´*-DDE intake increased GSR activity in testis tissue, mildly at 10 days of exposure, and significantly after 30 days treatment (Fig. 3B).

CAT is a haemoprotein that catalyses reduction of hydrogen peroxide, protecting cells from ROS. Induction of CAT enzymatic activity is generally provoked by increased ROS levels and, therefore, CAT is commonly used as a biomarker for

443 oxidative stress in many organisms. As a caveat, some studies have demonstrated in
444 rodents that free-radical generators, including *p,p´*-DDE, may act by decreasing levels
445 of antioxidative enzymes, including CAT, both *in vivo* (Gupta et al., 2013; Shi et al.,
446 2010; Zhou et al., 2014) and *in vitro* (Luo et al., 2016; Song et al., 2014a). Diminished
447 CAT enzymatic activity was also previously reported in *M. spretus* dwelling in
448 contaminated sites (Montes-Nieto et al., 2007; Ruíz-Laguna et al., 2001). The increased
449 proteolytic susceptibility of this enzyme following exposure to various oxidants or the
450 sensitivity of haeme to ROS have been proposed as plausible explanations (Grune et
451 al., 2003; Montes-Nieto et al., 2007).
452 Glutathione is a low molecular-weight thiol tripeptide that plays a key role in
453 antioxidative defences. We evaluated reduced and oxidized glutathione content in
454 testis tissue after *p,p´*-DDE treatments (Fig. 3C and Supplementary Fig. 1). Exposure to
455 *p,p´*-DDE caused moderate changes in GSSG/GSH ratio in mouse testis. Strikingly, initial
456 reduced and oxidized glutathione contents in control animals fluctuated even more so
457 than MDA values (Supplementary Fig. 1). However, similar to MDA measurements,
458 inter-individual glutathione variability seemed to smooth out in *p,p´*-DDE treated mice.
459 For that reason, although an increase in testis GSSG/GSH ratio was notable after 30-
460 day exposure to *p,p´*-DDE (Fig. 3C), the pollutant could not be significantly associated
461 with any general tendency due to high variability in the controls.
462 GSR reduces oxidized glutathione back to GSH at the expense of NADPH. The
463 pattern of GSR changes observed after *p,p´*-DDE treatment (Fig. 3B) was similar to the
464 variation seen in total glutathione content (Fig. 3C), suggesting common regulation of
465 both biochemical markers.
466

3.4 Post-translational modifications in mouse testis in response to p,p´-DDE exposure

Formation of carbonyl residues in proteins is an irreversible modification that depends on ROS levels and leads to protein degradation (McDonagh 2017). Recent advances in proteomics have prompted the adoption of carbonylation levels in proteins being used as an early biomarker for oxidation in several organisms. In this study, we observed a significant decline in the overall levels of protein carbonyls in mouse testis after both 10 and 30-days *p,p´*-DDE exposure (Fig. 4A, Supplementary Fig. 2). Previously, *p,p´*-DDE exposure has been linked to an increase in protein carbonylation in *Ruditapes decussatus* clams (Dowling 2006), but this correlation failed to be confirmed in other aquatic organisms (Vieira 2016). Our results could be due to protein degradation, as moderate oxidant levels increase degradation of damaged proteins, while high oxidation represses proteolysis (Grune et al., 2003). Hence, *p,p´*-DDE treatment in our mice may generate moderate oxidation levels able to stimulate damaged protein degradation, thus leading to the observed decrease in protein carbonyls.

Reversible phosphorylation of proteins is pivotal for cell signalling modulation in response to environmental stimuli (Humphrey et al., 2015; Olsen et al., 2006). We next evaluated the effect of *p,p´*-DDE exposure on overall protein phosphorylation after 1-D electrophoresis using the double Pro-Q Diamond/Sypro Ruby staining that specifically detects proteins with phosphate groups on serine, threonine, and tyrosine residues and allows normalization to global phosphorylation levels (Fig. 4B, Supplementary Fig. 2). Similar to carbonylated modifications, phosphorylated proteins revealed differences in mice testis exposed to *p,p´*-DEE *vs.* controls, with a global decrease of more than 20% in protein phosphorylation associated with *p,p´*-DDE

491 treatment. In testis, ROS-mediated protein Tyr phosphorylation has been previously
492 correlated with human sperm capacitation (Dona et al., 2010; Visconti et al., 2002). On
493 the other hand, increased oxidative stress in human spermatozoa has been linked to
494 infertility, a decrease in protein phosphotyrosine content and sperm motility (Dona et
495 al., 2010; Lachance et al., 2015; O'Flaherty and de Souza, 2011; Visconti et al., 2002).
496 Although the molecular mechanism underlying this signalling is not well understood,
497 tyrosine phosphatases contain an essential ROS sensitive cysteine residue in their
498 active motif that can modulate their activity (Rhee et al., 2005).
499 Cysteine residues are one of the less abundant amino acids, although they
500 usually play key functions in proteins (Eaton, 2006; Ying et al., 2007). Protein redox
501 modifications typically affect cysteine thiol groups that can undergo both reversible
502 and irreversible changes. Reversible formation of disulphide bonds is significantly
503 affected by ROS content and therefore can quickly influence the activity of an enzyme
504 or contribute to cellular signalling (Paulsen and Carroll, 2013). “Redox state” refers to
505 the ratio of the interconvertible oxidized and reduced forms of a redox couple, in our
506 case the thiol groups from the cysteine residues. To investigate the effect of *p,p´*-DDE
507 on the redox state of proteins in *M. spretus* testis, both reduced and oxidized Cys
508 residues were independently fluorescently labelled and their global levels quantified.
509 Fig. 4C represents the ratio between normalized global oxidized to reduced cysteine
510 levels in protein extracts from *p,p´*-DDE-exposed and control mouse testis (see also
511 Supplementary Fig. 2). As described previously for GSH, MDA and 8-OHdG, fluctuations
512 in the controls likely concealed possible differences in protein redox state in response
513 to *p,p´*-DDE treatment. Hence, despite obtained profiles indicating an increase in the

514 proportion of oxidized residues at 10 days followed by a decrease at 30 days, we could
515 not statistically confirm this.
516 Some of the results obtained in this work are not statistically significant due to
517 the presence of high variability in control mice. Although *M. spretus* is acknowledged
518 as a useful model for studying many disease-related mechanisms in humans, these
519 mice also present some disadvantages as they are aggressive, poor breeders and
520 sensitive to stress (Dejager et al., 2009). This sensitivity may provoke huge differences
521 in their biochemical stress responses. In inbreed Swiss albino mice, for example, large
522 heterogeneity in their anxiety levels has been described, as well as how those levels
523 could be related to intracellular ROS generation (Bouayed et al., 2007; Rammal et al.,
524 2008). The relation of oxidative stress and anxiety has also been widely documented in
525 humans (a recent review in (Krolow et al., 2014)). Indeed, perhaps small behavioural
526 changes led to the vast differences in certain oxidative parameters that we observed.
527 Intriguingly, those differences did not persist after exposure to *p,p´*-DDE, suggesting a
528 higher level of control for the measured parameters in the presence of this chemical
529 stressor.
530
531 *3.5 Redox analysis with differential isotopic cysteine labelling and global proteomics*
532 Reversible oxidoreduction in cysteines can act as a control point of protein
533 structure and function. As stated above, low levels of ROS are needed to activate the
534 function of human sperm; however, high levels can cause infertility (O'Flaherty and de
535 Souza, 2011). We implemented a high-throughput proteomic approach using LC-
536 MS/MS analysis to identify and quantify the reversible redox state of specific Cys
537 residues in peptides. To that end, reduced and oxidized cysteine residues were

differentially labelled with the isotopic light (d0) and heavy (d5) forms of NEM, respectively. Proteins obtained from testis exposed or not to *p,p´*-DDE were differentially labelled and tryptic digested as explained in section 2.6. The resulting peptides were analysed by LC-MS/MS. Peptides containing Cys labelled with both d(0) and d(5) NEM were quantified and selected for further analysis. Using this approach, the analysis of testes from *p,p´*-DDE exposed mice revealed that the redox state of Cys residues was affected by exposure to *p,p´*-DDE (Fig. 4). Up to 112 peptides presenting both d(0) NEM modifications, corresponding to reduced Cys residues, and d(5) NEM modifications, corresponding to oxidized Cys residues, were selected for this study in all three conditions (control, DDE10 and DDE30). Using Genesis software, hierarchical clustering analysis of differentially oxidized peptides was performed to evaluate the relationship between Cys oxidation and exposure in mouse testis. Peptides were distributed in four groups according to their oxidation pattern after exposure to the pollutant (Fig. 5). The largest cluster contains proteins with a peak of oxidation at DDE10 (pattern C) that agrees with the global redox oxidation state shown in section 3.4, Fig. 4C. Most of the identified peptides, 89 out of 112 (Fig. 5; patterns A, C and D) showed an increase in oxidized/reduced Cys redox state upon *p,p´*-DDE exposure. These differences were observed either at 10 days (pattern C), 30 days (pattern A), or at both times (pattern D), consistent with an increase in protein oxidation. These results are in agreement with previous reports of ROS generation in response to this pollutant (Harada et al., 2016; Li et al., 2017; Morales-Prieto and Abril, 2017; Morales-Prieto et al., 2017).

The 112 peptides containing differentially oxidized cysteines belong to 77 different proteins (Table 1). To assign biological functions to the identified proteins,

562 ClueGo was used to obtain an overview chart showing the main groups and their
563 leading terms (Fig. 6). Twenty-two of the proteins with an altered redox state were
564 connected to male fertility (single fertilization and sperm capacitation were the leading
565 terms). Fourteen were related to oxidative stress (cell redox homeostasis, cellular
566 transition metal ion homeostasis) and oxidative phosphorylation, and four were
567 involved in negative regulation of blood coagulation as leading terms. Other processes
568 affected included protein folding and positive regulation of nucleotide biosynthetic
569 processes or endocytosis (Fig. 6).

570 Although the molecular functions of several proteins whose peptides exhibited
571 oxidized Cys in response to *p,p´*-DDE were unknown, among those previously
572 described in the literature, several play pivotal roles in reproduction. Nuclear transition
573 protein 2 (STP2) participates in chromatin remodelling during spermatogenesis, an
574 essential step for functional sperm production (Zhao et al., 2004). Inactive
575 ribonuclease-like protein 10 (RNS10) contributes to spermatozoa adhesiveness,
576 although, male mice with the Rnse10 gene disrupted were shown to possess superior
577 fertilization rates *in vitro* due to higher capacitation (Krutskikh et al., 2012).
578 Arylsulfatase A (ARSA) regulates sulfogalactosylglycerolipid degradation in Sertoli cells,
579 preventing lysosomal disorders in sperm (Xu et al., 2011). Finally, sperm acrosome
580 membrane-associated protein 3 (SACA3) is a lysozyme-like protein localized in the
581 acrosomal matrix that plays an important role in mouse fertilization (Ito and Toshimori,
582 2016).

583 Although exposure to *p,p´*-DDE has been linked to an increase in ROS (Song et
584 al., 2011) and most of the peptides analysed in this work increased their oxidation in
585 *p,p´*-DDE fed mice, 23 peptides exhibited the opposite result (Fig. 5, pattern B).

586 Furthermore, according to a Uniprot database, 13 of these 23 peptides were attributed
587 to 11 proteins that are also functionally linked to male fertility, particularly to
588 capacitation of mammalian spermatozoa: Heat shock 70 KDa protein 1-like (HS71l),
589 dipeptidase 3 (DPEP3), acrosin-binding protein (ACRBP), dihydrolipoyl dehydrogenase
590 (DLDH), testis-expressed protein 101 (TEX101), β-hexosaminidase subunit β (HEXb),
591 serine protease inhibitor kazal-type 2 (ISK2), serine protease inhibitor kazal-like protein
592 (SPIKL), trypsin-like protease acrosin (ACRO), sperm acrosome membrane-associated
593 protein 1 (SACA1), and La-related protein 7 (LARP7) (Fig. 5 and Table 1). In mature
594 mouse testis extracts, DPEP3 acts as a disulphide-linker homodimer that forms
595 complexes with TEX101, and together they play a role in sperm cell differentiation
596 (Yoshitake et al., 2011). The exact function of both proteins is still unknown, although
597 TEX101 is required for proper localization of cyritestin ADAM3 on the mature sperm
598 surface (Liu, 2016). Furthermore, TEX101 is regulated by angiotensin converting
599 enzyme (ACE), another of the proteins identified in this study, that also exhibited
600 notable reduction after 30 days *p,p´*-DDE exposure (Fig. 5, pattern C) and is linked to
601 capacitation as well (Fujihara et al., 2013). ACRBP may play a pivotal role in the
602 transport/packing of pro-ACR into acrosomal granules during spermatogenesis
603 (Kanemori et al., 2013). DLDH is a flavoenzyme oxidoreductase with a reactive
604 disulphide bridge directly involved in catalysis (the formation of homodimers is
605 required for its enzymatic activity) (Ciszak et al., 2006). HEX is an essential lysosomal
606 enzyme found in the acrosome that facilitates sperm penetration (Juneja, 2002; Miller
607 et al., 1993). Furthermore, both ACRBP and DLDH require tyrosine phosphorylation for
608 sperm capacitation (Kanemori et al., 2013; Mitra et al., 2005), while aggregation of a
609 TEX101 homologue in rats induces Tyr phosphorylation (Halova et al., 2002). ACRO is

610 the major proteinase present in the acrosome. It is synthesized as proacrosin and,
611 upon stimulation, is processed into its active form, facilitating fecundation (Tranter et
612 al., 2000). Both ISK2 and its homologue SPIKL inhibit premature early capacitation, ISK2
613 directly by preventing proacrosin autoactivation (Kherraf et al., 2017; Lin et al., 2008).
614 Finally, SACA1 is an acrosomal membrane protein essential for sperm-egg fusion that
615 possesses a potential Tyr phosphorylation site (Fujihara et al., 2012). The majority of
616 these proteins form homo- or hetero-complexes. Thus, we speculate that targeted Cys
617 reduction could prevent the interactions between these proteins, altering their
618 functionality.

619 On the other hand, only 24 peptides presented a clear increased in their Cys
620 oxidation status both at 10 and 30 days of *p,p´*-DDE exposure (Fig. 5, pattern D) but
621 they are not mainly associated to any particular biological function. Furthermore some
622 proteins related to reproduction follow this pattern (*i.e.* arylsulfatase A (ARSA), CUB
623 and zona pellucida-like (CUZB1) or RNA-binding protein (FUS)). These results may
624 suggest that not all proteins linked to reproduction are specifically protected to
625 oxidation upon *p,p´*-DDE exposure.

626 The oxidation status of Cys in peptides was also altered in proteins involved in
627 negative regulation of blood coagulation, i.e.: calreticulin, fibrinogen gamma chain,
628 HMW kininogen-II and plasminogen. In humans, immediately after ejaculation, a
629 process called coagulation and liquefaction “fibrinolysis” causes semen to form a gel-
630 like coagulum that subsequently spontaneously liquefies. This process, mediated
631 through the high molecular weight seminal vesicles (HMW-SV) proteins system, is
632 known to play a major role in sperm capacitation (Fernandez and Heeb, 2007; Lwaleed

et al., 2007; Lwaleed et al., 2004). In summary, changes in the redox state of proteins involved in blood coagulation could compromise male fertility.

As previously mentioned, several proteins related to oxidative stress exhibited changes in their oxidation status in response to *p,p´*-DDE treatment, including peroxiredoxin (PRDX), glutathione S-transferases, thioredoxins, etc. Increased thiol oxidation of PRDX1, but not of PRDX5, has been previously linked to oxidative stress in human spermatozoa (Gong et al., 2012; O'Flaherty and de Souza, 2011). Most of these proteins presented an increment in their oxidation upon *p,p´*-DDE exposure that peaked at 10 days (ARK72, GSTM6, GSTM7, LDH, PRXD1, PDIA5 or TXND5).

One of the limitations of this technique is a low sensitivity in detecting scarce proteins, even if their Cys residues undergo drastic redox changes that could only be avoided by a direct search for specific peptide targets (McDonagh, 2017). A second limitation involves instances in which more than one peptide identifies the same protein and yet resulting in different behaviours (i.e., serotransferrin (TRFE) and serum albumin (ALBU) were identified from seven and five peptides, respectively; most of them (4 peptides in TRFE and 3 in ALBU) following pattern A, two following pattern D, and the last one included in pattern C. Regardless of pattern, however, increases in Cys oxidation status in response to *p,p´*-DDE exposure was observed in all three patterns. The explanation for this hypothetical inconsistency may be explained by the fact that not all Cys residues within a protein are equally exposed to oxidation, as their reactivity to ROS is strongly influenced by their micro-surroundings (Morales-Prieto and Abril, 2017; Paulsen and Carroll, 2013). Sulfhydryl residues in the same protein can have differences in their *pKa* values (up to 6.5 units), and, theoretically, only low *pKa* Cys will be sensitive to ROS, although the explanation for this variation in redox

sensitivity is still under investigation (Paulsen and Carroll, 2013). Nevertheless, as proteins in this work were identified heterologously using the *Mus musculus* library, the existence of inaccurate peptide assignations cannot be excluded.

To rule out if the differences detected in this study could be influenced by changes in the overall protein abundance, a label-free quantitative proteomics analysis was carried out. *p,p´*-DDE did not substantially change the expression of proteins with an altered oxidation Cys pattern, as only two proteins (HEXb and FAM3C) increased their concentration more than 2-fold upon *p,p´*-DDE exposure (Supplementary Table 1). We may highlight that in the reproduction-related HEXb, global protein abundance increases although its Cys oxidation levels decrease upon exposure to the pollutant. Overall, the absence of changes in protein expression suggests that the modifications in state of Cys residues are an specific redox signalling effect.

Although ROS at low levels act as secondary messengers in processes as sperm capacitation or acrosome reaction (Bui et al., 2018), several studies have linked excess ROS to male infertility (for recent reviews see (Bisht et al., 2017)). Sperm is highly sensitive to oxidative stress due to their low levels of antioxidants and DNA repair mechanisms (Bisht et al., 2017). Furthermore, oxidative stress decreases sperm mobility and the ability to fuse with the oocyte (Fujii and Tsunoda, 2011). Disulfhydryl bond formation in protamines of mammalian sperm, among other ROS-mediate signals, have been proposed for the understanding of redox regulation of the reproductive process (Fujii and Tsunoda, 2011). As stated in this work, this mechanism clearly affects more proteins involved in reproduction.

4. Conclusions

p,p´-DDE is an endocrine-disruptor that has been epidemiologically linked to severe reproductive disorders in animals and human beings although the underlying mechanisms are not clearly understood. Previous studies reported that *p,p´*-DDE exposure generates oxidative stress. We observed changes in the antioxidative response of mouse testis in response to oxidative stress generated by *p,p´*-DDE, i.e*.,* an increase of glutathione reductase and total glutathione, accompanied by a decrease in catalase activity. Cellular protection mechanisms try to avoid excessive damage to biomolecules and at higher levels. In mammals, testes are additionally protected against external insult by the blood-testis barrier. In testis, *p,p´*-DDE does not oxidatively damage lipids (MDA), DNA (8-OHdG) or proteins (carbonylation), whose levels were actually even lower after exposure, significantly in the case of the irreversible carbonylation of proteins. The histological analysis did not reveal apparent damages to the capability of seminiferous tubules to produce spermatozoids.

The testes are the most essential organs of the male reproductive system and maintaining their integrity and functionality is critical for preserving their reproductive capacity. In response to oxidative stress, proteins absorb the bulk of ROS, resulting in reversible, targeted modifications that respond dynamically similar to an on-off switch. The decrease in global protein phosphorylation levels observed in this work could be an adaptive response contributing to modulating their functions, with consequences in signal transduction, regulatory and metabolic pathways. As already indicated, Cys is a key residue that is especially vulnerable to many electrophiles like ROS due to its unique redox properties. Although the global oxidation state of protein thiol groups was not drastically altered in testis in response to *p,p´*-DDE, detailed analysis with differential isotopic labelling and global proteomics revealed changes in specific Cys

residues of relevant proteins that were primarily related to oxidative stress and reproduction. Thus, cell redox homeostasis may be altered due to changes in the oxidation state of proteins including glutathione S-transferases Mu 6 and 7, peroxiredoxins 1 and 5, and thioredoxins. Significantly, the largest functional group exhibiting changes in the oxidation state of Cys-containing proteins due to *p,p´*-DDE is related to single fertilization and sperm capacitation, which could explain the negative consequences of this organochlorine pesticide on male fertility. Changes in the redox state of proteins involved in the negative regulation of blood coagulation may cause alterations in the coagulation/liquefaction processes and thus additionally compromise male fertility. The oxido-reduction of specific Cys thiols can have two opposing consequences: i) reversible oxidation may protect protein thiols from irreversible oxidation and reprogram metabolism during oxidative stress, ii) oxidation could negatively alter protein structure, function, or redox signalling. Further studies are required to determine the precise consequences of redox alteration for each protein.

Figure legends

Fig. 1. Histopathological analysis of control and *p,p´*-DDE-treated mice. (A) Testis of control mice showing normal histological structure of seminiferous tubules; SP: spermatocytes; ST: spermatids; SZ: spermatozoa. (B & C) Testis of *p,p´*-DDE-treated mice after 10 and 30 days, respectively. H&E staining; 40X magnification.

Fig. 2. Changes in MDA (A) and 8-OHdG (B) concentrations as biomarkers of for oxidative damage to lipids and DNA, respectively, caused by *p,p´*-DDE mice exposure in mice for 10 (DDE10) and 30 days (DDE30) compared with 30 days of no exposure in

control animals. Bars on the left represent the mean ± SD of at least three independent determinations in each of the four independent mice per exposure time, while bars on the right represent average values of the four mice per condition.

Fig. 3. Changes in antioxidant enzyme activity of catalase (A) and glutathione reductase (B), and GSSG/GSH ratio (C) in response to *p,p´*-DDE treatment for 10 (DDE10) and 30 days (DDE30) compared with 30 days untreated control animals. Further description as in Fig. 2. Statistically significant differences are expressed as **, $p < 0.01$, ***, $p < 0.001$.

Fig. 4. Electrophoresis-based evaluation of post-translational modification levels in testes of mice exposed to *p,p´*-DDE for 10 (DDE10) and 30 days (DDE30) compared with 30 days untreated control animals. Carbonylation (A), phosphorylation (B) and the redox state of cysteine (oxidized/reduced) residues (C) in proteins are shown. Further description as in Fig. 2. Statistically significant differences are expressed as *, $p < 0.05$.

Fig. 5. Cluster analysis of differentially oxidized cysteine (Cys)-containing peptides in mouse testis after exposure to *p,p´*-DDE for 10 (DDE10) and 30 days (DDE30) compared with 30 days untreated control animals (left). Columns represent the oxidation profile (oxidized/reduced Cys redox state) of each condition. Each row represents one differentially oxidized Cys-containing peptide. Green rectangles indicate samples with lower Cys-oxidation level for the respective peptide relative to other conditions, and red rectangles represent higher oxidation levels. The colour intensity is proportional to the fold-change as represented by the scale. Peptides are grouped into four clusters (A-D) whose trend is shown in the graphs on the left, indicating the number of peptides that comprise each cluster.

751 **Fig. 6.** Overview chart with functional groups, including specific terms for the proteins
752 identified as exhibiting differentially oxidized cysteine-containing peptides.

753

754 **Supplementary Figure legends**

755 **Supplementary Fig. 1.** Changes in reduced (GSH) and (GSSG) oxidized glutathione in
756 response to *p,p´*-DDE treatment for 10 (DDE10) and 30 days (DDE30) compared with
757 30 days untreated control animals. Bars on the left represent the mean ± SD in each of
758 the four independent mice per exposure time, while bars on the right represent
759 average values of the four mice per condition.

760 **Supplementary Fig. 2.** Representative gels for post-translational modification
761 determinations. (A) Carbonylation, (B) phosphorylation, (C) and (D) redox state of Cys
762 (oxidized/reduced) residues images are shown. In (A) and (B), lanes 1-4 correspond to
763 the four control individuals, and lanes 5-8 to mice exposed to *p,p´*-DDE for 30 (DDE30).
764 In (C) and (D), lanes 1-4 correspond to reduced thiols in proteins from controls (C), and
765 DDE30 (D) mice and lanes 5-8 to the oxidized ones.

766

767 **Acknowledgements**

768 We would like to express our sincere thanks to Dr. Ricardo Fernández-Cisnal,
769 Dr. Eduardo Chicano, Prof. José Antonio Bárcena and Dr. Brian McDonagh for helping
770 in label-based proteomic experiments and analysis, and Prof. Juan López-Barea and
771 Prof. Carmen Pueyo for critical reading the MS. We also thank Dr. Noelia Morales-
772 Prieto and the SAEX-UCO staff their help with the *p,p´*-DDE exposure experiments and
773 sample preparation and to Isabel L. Pacheco and Prof. José Pérez for helping with the

774 histopathological analysis of testes samples. The study was supported by the European
775 Regional Development Fund, the Spanish Ministry of Economy and Competitiveness
776 (MINECO, CTM2012-38720-C03-02 and CTM2015-67902-C2-1-P), the Agency of
777 Economy, Competitiveness, Science, and Employment of the Andalusian Government
778 (BIO1657) and by the Andalusian Plan of Research, Development, and Innovation
779 (PAIDI) to group BIO187. Mice experiments were performed at the UCO-SAEX
780 (Centralized Animal Experimentation Service, University of Cordoba). The mass
781 spectrometry analyses were carried out in the UCO-SCAI (Centralized Research Support
782 Proteomic facility, University of Cordoba).

783

784 **References**

785 Abril N, Chicano-Galvez E, Michan C, Pueyo C, Lopez-Barea J. iTRAQ analysis of hepatic proteins
786 in free-living *Mus spretus* mice to assess the contamination status of areas surrounding
787 Donana National Park (SW Spain). Sci Total Environ 2015;523:16-27.
788 Alvarez-Pedrerol M, Ribas-Fito N, Torrent M, Carrizo D, Grimalt JO, Sunyer J. Effects of PCBs,
789 *p,p'*-DDT, *p,p'*-DDE, HCB and beta-HCH on thyroid function in preschool children.
790 Occup Environ Med 2008;65:452-7.
791 Aulakh RS, Bedi JS, Gill JP, Joia BS, Pooni PA, Sharma JK. Occurrence of DDT and HCH insecticide
792 residues in human biopsy adipose tissues in Punjab, India. Bull Environ Contam Toxicol
793 2007;78:330-4.
794 Bindea G, Mlecnik B, Hackl H, Charoentong P, Tosolini M, Kirilovsky A, et al. ClueGO: a
795 Cytoscape plug-in to decipher functionally grouped gene ontology and pathway
796 annotation networks. Bioinformatics 2009;25:1091-3.
797 Bisht S, Faiq M, Tolahunase M, Dada R. Oxidative stress and male infertility. Nat Rev Urol 2017;
798 14:470-485.

799 Bonilla-Valverde D, Ruiz-Laguna J, Munoz A, Ballesteros J, Lorenzo F, Gomez-Ariza JL, et al.
800 Evolution of biological effects of Aznalcollar mining spill in the Algerian mouse (*Mus*
801 *spretus*) using biochemical biomarkers. Toxicology 2004;197:123-38.
802 Bouayed J, Rammal H, Younos C, Soulimani R. Positive correlation between peripheral blood
803 granulocyte oxidative status and level of anxiety in mice. Eur J Pharmacol 2007;564:
804 146-9.
805 Brown RK, Kelly FJ. Peroxides and other products. In Punchard NA, Kelly FJ, eds, Free Radicals.
806 A Practical Approach. IRL Press, Oxford, UK 1996: 119-31.
807 Bui AD, Sharma R, Henkel R, Agarwal A. Reactive oxygen species impact on sperm DNA and its
808 role in male infertility. Andrologia 2018:e13012.
809 Cabiscol E, Ros J. Oxidative damage to proteins: structural modifications and consequences in
810 cell function. In: Dalle-Donne I, Scaloni A, Butterfield DA, editors. Redox Proteomics:
811 From Protein Modifications to Cellular Dysfunction and Diseases. John Wiley & Sons,
812 Inc., Hoboken, New Jersey, USA, 2006, p399-471.
813 Ciszak EM, Makal A, Hong YS, Vettaikkorumakankauv AK, Korotchkina LG, Patel MS. How
814 dihydrolipoamide dehydrogenase-binding protein binds dihydrolipoamide
815 dehydrogenase in the human pyruvate dehydrogenase complex. J Biol Chem 2006;
816 281: 648-55.
817 Cox J, Hein MY, Luber CA, Paron I, Nagaraj N, Mann M. Accurate proteome-wide label-free
818 quantification by delayed normalization and maximal peptide ratio extraction, termed
819 MaxLFQ. Mol Cell Proteomics 2014;13:2513-26.
820 Cox J, Mann M. MaxQuant enables high peptide identification rates, individualized p.p.b.-range
821 mass accuracies and proteome-wide protein quantification. Nat Biotechnol 2008;26:
822 1367-72.

823 Chaudhuri AR, de Waal EM, Pierce A, Van Remmen H, Ward WF, Richardson A. Detection of
824 protein carbonyls in aging liver tissue: A fluorescence-based proteomic approach.
825 Mech Ageing Dev 2006;127:849-61.
826 Davies MJ. The oxidative environment and protein damage. Biochim Biophys Acta 2005;1703:
827 93-109.
828 Daxenberger A. Pollutants with androgen-disrupting potency Eur. J. Lipid Sci. Technol. 2002;
829 104:124-130.
830 Dejager L, Libert C, Montagutelli X. Thirty years of *Mus spretus*: a promising future. Trends
831 Genet 2009;25:234-41.
832 Dejager L, Pinheiro I, Puimege L, Fan YD, Gremeaux L, Vankelecom H, et al. Increased
833 glucocorticoid receptor expression and activity mediate the LPS resistance of SPRET/EI
834 mice. J Biol Chem 2010;285:31073-86.
835 Dona G, Fiore C, Tibaldi E, Frezzato F, Andrisani A, Ambrosini G, et al. Endogenous reactive
836 oxygen species content and modulation of tyrosine phosphorylation during sperm
837 capacitation. Int J Androl 2010;34:411-9.
838 Dowling V, Hoarau PC, Romeo M, O'Halloran J, van Pelt F, O'Brien N, et al. Protein
839 carbonylation and heat shock response in *Ruditapes decussatus* following *p,p'*-
840 dichlorodiphenyldichloroethylene (DDE) exposure: a proteomic approach reveals that
841 DDE causes oxidative stress. Aquat Toxicol 2006;77:11-8.
842 Eaton P. Protein thiol oxidation in health and disease: techniques for measuring disulfides and
843 related modifications in complex protein mixtures. Free Radic Biol Med 2006;40:1889-
844 99.
845 Fernandez-Cisnal R, Alhama J, Abril N, Pueyo C, Lopez-Barea J. Redox proteomics as biomarker
846 for assessing the biological effects of contaminants in crayfish from Donana National
847 Park. Sci Total Environ 2014;490:121-33.

848 Fernandez JA, Heeb MJ. Role of protein C inhibitor and tissue factor in fertilization. Semin
849 Thromb Hemost 2007;33:13-20.
850 Fujihara Y, Satouh Y, Inoue N, Isotani A, Ikawa M, Okabe M. SPACA1-deficient male mice are
851 infertile with abnormally shaped sperm heads reminiscent of globozoospermia.
852 Development 2012;139:3583-9.
853 Fujihara Y, Tokuhiro K, Muro Y, Kondoh G, Araki Y, Ikawa M, et al. Expression of TEX101,
854 regulated by ACE, is essential for the production of fertile mouse spermatozoa. Proc
855 Natl Acad Sci U S A 2013;110:8111-6.
856 Fujii J, Tsunoda S. Redox regulation of fertilisation and the spermatogenic process. Asian J
857 Androl 2011;13:420-3.
858 Garcia-Sevillano MA, Garcia-Barrera T, Abril N, Pueyo C, Lopez-Barea J, Gomez-Ariza JL. Omics
859 technologies and their applications to evaluate metal toxicity in mice *M. spretus* as a
860 bioindicator. J Proteomics 2014;104:4-23.
861 Geric M, Ceraj-Ceric N, Gajski G, Vasilic Z, Capuder Z, Garaj-Vrhovac V. Cytogenetic status of
862 human lymphocytes after exposure to low concentrations of *p,p'*-DDT, and its
863 metabolites (*p,p'*-DDE, and *p,p'*-DDD) in vitro. Chemosphere 2012;87:1288-94.
864 Ghedira J, Jebali J, Banni M, Chouba L, Boussetta H, López-Barea J, et al. Response of oxidative
865 stress biomar-kers in *Carcinus maenas* crabs from areas of Tunisian Coast and to
866 controlled exposure to cadmium and chlorpyrifos-ethyl. Aquat Biol 2011;14:87-98.
867 Gong S, San Gabriel MC, Zini A, Chan P, O'Flaherty C. Low amounts and high thiol oxidation of
868 peroxiredoxins in spermatozoa from infertile men. J Androl 2012;33:1342-51.
869 Graves JD, Krebs EG. Protein phosphorylation and signal transduction. Pharmacol Ther 1999;
870 82:111-21.
871 Gray LE, Jr., Kelce WR. Latent effects of pesticides and toxic substances on sexual
872 differentiation of rodents. Toxicol Ind Health 1996;12:515-31.

873 Grune T, Merker K, Sandig G, Davies KJ. Selective degradation of oxidatively modified protein
874 substrates by the proteasome. Biochem Biophys Res Commun 2003;305:709-18.
875 Gupta P, Bansal MP, Koul A. Lycopene modulates initiation of N-nitrosodiethylamine induced
876 hepatocarcinogenesis: Studies on chromosomal abnormalities, membrane fluidity and
877 antioxidant defense system. Chem Biol Interact 2013;206:364-374.
878 Gutteridge JM. Ferrous ion-EDTA-stimulated phospholipid peroxidation. A reaction changing
879 from alkoxyl-radical- to hydroxyl-radical-dependent initiation. Biochem J 1984; 224:
880 697-701.
881 Halova I, Draberova L, Draber P. A novel lipid raft-associated glycoprotein, TEC-21, activates rat
882 basophilic leukemia cells independently of the type 1 Fc epsilon receptor. Int Immunol
883 2002;14:213-23.
884 Harada T, Takeda M, Kojima S, Tomiyama N. Toxicity and Carcinogenicity of
885 Dichlorodiphenyltrichloroethane (DDT). Toxicol Res 2016;32:21-33.
886 Humphrey SJ, James DE, Mann M. Protein Phosphorylation: A Major Switch Mechanism for
887 Metabolic Regulation. Trends Endocrinol Metab 2015;26:676-87.
888 Ito C, Toshimori K. Acrosome markers of human sperm. Anat Sci Int 2016; 91: 128-42.
889 Juneja SC. Development of infertility at young adult age in a mouse model of human Sandhoff
890 disease. Reprod Fertil Dev 2002;14:407-12.
891 Kanemori Y, Ryu JH, Sudo M, Niida-Araida Y, Kodaira K, Takenaka M, et al. Two functional
892 forms of ACRBP/sp32 are produced by pre-mRNA alternative splicing in the mouse.
893 Biol Reprod 2013;88:105.
894 Kelce WR, Stone CR, Laws SC, Gray LE, Kemppainen JA, Wilson EM. Persistent DDT metabolite
895 *p,p'*-DDE is a potent androgen receptor antagonist. Nature 1995;375:581-5.
896 Kherraf ZE, Christou-Kent M, Karaouzene T, Amiri-Yekta A, Martinez G, Vargas AS, et al. SPINK2
897 deficiency causes infertility by inducing sperm defects in heterozygotes and
898 azoospermia in homozygotes. EMBO Mol Med 2017;9:1132-1149.

899 Krolow R, Arcego DM, Noschang C, Weis SN, C. D. Oxidative imbalance and anxiety disorders.
900 Curr Neuropharmacol 2014;12:193-204.
901 Krutskikh A, Poliandri A, Cabrera-Sharp V, Dacheux JL, Poutanen M, Huhtaniemi I. Epididymal
902 protein Rnase10 is required for post-testicular sperm maturation and male fertility.
903 Faseb J 2012;26:4198-209.
904 Lachance C, Goupil S, Tremblay RR, Leclerc P. The immobilization of human spermatozoa by
905 STAT3 inhibitory compound V results from an excessive intracellular amount of
906 reactive oxygen species. Andrology 2015;4:133-42.
907 Levine RL. Carbonyl modified proteins in cellular regulation, aging, and disease. Free Radic Biol
908 Med 2002;32:790-6.
909 Li K, Zhu X, Wang Y, Zheng S, Dong G. Effect of aerobic exercise intervention on DDT
910 degradation and oxidative stress in rats. Saudi J Biol Sci 2017;24:664-671.
911 Lin MH, Lee RK, Hwu YM, Lu CH, Chu SL, Chen YJ, et al. SPINKL, a Kazal-type serine protease
912 inhibitor-like protein purified from mouse seminal vesicle fluid, is able to inhibit sperm
913 capacitation. Reproduction 2008;136:559-71.
914 Liu M. Capacitation-Associated Glycocomponents of Mammalian Sperm. Reprod Sci 2016;23:
915 572-94.
916 López-Barea J. Biomarkers in ecotoxicology: an overview. In: Degen GH, Seiler JP, Bentely P,
917 editors. Toxicology in Transition. Springer, Berlin, 1995,p.57-79.
918 Lopez-Carrillo L, Torres-Arreola L, Torres-Sanchez L, Espinosa-Torres F, Jimenez C, Cebrian M,
919 et al. Is DDT use a public health problem in Mexico? Environ Health Perspect 1996;
920 104:584-8.
921 Luo G, Li Z, Wang Y, Wang H, Zhang Z, Chen W, et al. Resveratrol Protects against Titanium
922 Particle-Induced Aseptic Loosening Through Reduction of Oxidative Stress and
923 Inactivation of NF-kappaB. Inflammation 2016;39:775-85.

924 Lwaleed BA, Goyal A, Delves GH, Cooper AJ. Seminal hemostatic factors: then and now. Semin
925 Thromb Hemost 2007;33:3-12.
926 Lwaleed BA, Greenfield R, Stewart A, Birch B, Cooper AJ. Seminal clotting and fibrinolytic
927 balance: a possible physiological role in the male reproductive system. Thromb
928 Haemost 2004;92:752-66.
929 McDonagh B. Detection of ROS Induced Proteomic Signatures by Mass Spectrometry. Front
930 Physiol 2017;8:470.
931 McDonagh B, Sakellariou GK, Smith NT, Brownridge P, Jackson MJ. Differential cysteine
932 labeling and global label-free proteomics reveals an altered metabolic state in skeletal
933 muscle aging. J Proteome Res 2014;13:5008-21.
934 Messaros BM, Rossano MG, Liu G, Diamond MP, Friderici K, Nummy-Jernigan K, et al. Negative
935 effects of serum p,p'-DDE on sperm parameters and modification by genetic
936 polymorphisms. Environ Res 2009;109:457-64.
937 Miller DJ, Gong X, Shur BD. Sperm require beta-N-acetylglucosaminidase to penetrate through
938 the egg zona pellucida. Development 1993;118:1279-89.
939 Mitra K, Rangaraj N, Shivaji S. Novelty of the pyruvate metabolic enzyme dihydrolipoamide
940 dehydrogenase in spermatozoa: correlation of its localization, tyrosine
941 phosphorylation, and activity during sperm capacitation. J Biol Chem 2005;280:25743-
942 53.
943 Montes-Nieto R, Fuentes-Almagro CA, Bonilla-Valverde D, Prieto-Alamo MJ, Jurado J, Carrascal
944 M, et al. Proteomics in free-living *Mus spretus* to monitor terrestrial ecosystems.
945 Proteomics 2007;7:4376-87.
946 Montes Nieto R, Garcia-Barrera T, Gomez-Ariza JL, Lopez-Barea J. Environmental monitoring of
947 Domingo Rubio stream (Huelva Estuary, SW Spain) by combining conventional
948 biomarkers and proteomic analysis in *Carcinus maenas*. Environ Pollut 2010;158:401-8.

949 Morales-Prieto N, Abril N. REDOX proteomics reveals energy metabolism alterations in the
950 liver of *M. spretus* mice exposed to *p, p'*-DDE. Chemosphere 2017;186:848-863.
951 Morales-Prieto N, Pueyo C, Abril N. Validation of commercial real-time PCR-arrays for
952 environmental risk assessment: Application to the study of *p,p* -DDE toxicity in *Mus*
953 *spretus* mice liver. Environ Pollut 2017;230:178-188.
954 O'Flaherty C, de Souza AR. Hydrogen peroxide modifies human sperm peroxiredoxins in a
955 dose-dependent manner. Biol Reprod 2011;84:238-47.
956 Olsen JV, Blagoev B, Gnad F, Macek B, Kumar C, Mortensen P, et al. Global, *in vivo*, and site-
957 specific phosphorylation dynamics in signaling networks. Cell 2006;127:635-48.
958 Paulsen CE, Carroll KS. Cysteine-mediated redox signaling: chemistry, biology, and tools for
959 discovery. Chem Rev 2013;113:4633-79.
960 Perez-Maldonado IN, Athanasiadou M, Yanez L, Gonzalez-Amaro R, Bergman A, Diaz-Barriga F.
961 DDE-induced apoptosis in children exposed to the DDT metabolite. Sci Total Environ
962 2006;370:343-51.
963 Quan C, Shi Y, Wang C, Wang C, Yang K. p,p'-DDE damages spermatogenesis via phospholipid
964 hydroperoxide glutathione peroxidase depletion and mitochondria apoptosis pathway.
965 Environ Toxicol 2016;31:593-600.
966 Rammal H, Bouayed J, Younos C, Soulimani R. Evidence that oxidative stress is linked to
967 anxiety-related behaviour in mice. Brain Behav Immun 2008;22:1156-9.
968 Rhee SG, Kang SW, Jeong W, Chang TS, Yang KS, Woo HA. Intracellular messenger function of
969 hydrogen peroxide and its regulation by peroxiredoxins. Curr Opin Cell Biol 2005;17:
970 183-9.
971 Rivero-Rodriguez L, Borja-Aburto VH, Santos-Burgoa C, Waliszewskiy S, Rios C, Cruz V.
972 Exposure assessment for workers applying DDT to control malaria in Veracruz, Mexico.
973 Environ Health Perspect 1997;105:98-101.

974 Rodriguez-Ariza A, Abril N, Navas JI, Dorado G, Lopez-Barea J, Pueyo C. Metal, mutagenicity,
975 and biochemical studies on bivalve molluscs from Spanish coasts. Environ Mol
976 Mutagen 1992;19:112-24.
977 Rodriguez-Ariza A, Martinez-Lara E, Pascual P, Pedrajas JR, Abril N, Dorado G, et al. Biochemical
978 and genetic indices of marine pollution in Spanish littoral. Sci Total Environ 1993;Suppl
979 Pt 1:109-16.
980 Rogan WJ, Chen A. Health risks and benefits of bis(4-chlorophenyl)-1,1,1-trichloroethane
981 (DDT). Lancet 2005;366:763-73.
982 Ruíz-Laguna J, García-Alfonso C, Peinado J, Moreno S, Ieradi L, Cristaldi M, et al. Biochemical
983 biomarkers of pollution in Algerian mouse (*Mus spretus*) to assess the effects of
984 Aznalcollar disaster on Doñana Park (Spain). Biomarkers 2001;6:146-160.
985 Schilling B, Rardin MJ, MacLean BX, Zawadzka AM, Frewen BE, Cusack MP, et al. Platform-
986 independent and label-free quantitation of proteomic data using MS1 extracted ion
987 chromatograms in skyline: application to protein acetylation and phosphorylation. Mol
988 Cell Proteomics 2012;11:202-14.
989 Sheehan D, McDonagh B, Barcena JA. Redox proteomics. Expert Rev Proteomics 2010; 7: 1-4.
990 Shi Y, Song Y, Wang Y, Liang X, Hu Y, Guan X, et al. *p,p'*-DDE induces apoptosis of rat Sertoli
991 cells via a FasL-dependent pathway. J Biomed Biotechnol 2009;2009:181282.
992 Shi YQ, Li HW, Wang YP, Liu CJ, Yang KD. p,p'-DDE induces apoptosis and mRNA expression of
993 apoptosis-associated genes in testes of pubertal rats. Environ Toxicol 2011;28:31-41.
994 Shi YQ, Wang YP, Song Y, Li HW, Liu CJ, Wu ZG, et al. *p,p'*-DDE induces testicular apoptosis in
995 prepubertal rats via the Fas/FasL pathway. Toxicol Lett 2010;193:79-85.
996 Sies H. Biochemistry of oxidative stress. Angew Chem Int Ed Engl 1986;25:1058-71.
997 Song L, Liu J, Jin X, Li Z, Zhao M, Liu W. *p,p'*-Dichlorodiphenyldichloroethylene induces
998 colorectal adenocarcinoma cell proliferation through oxidative stress. PLoS One 2014a;
999 9:e112700.

1000 Song Y, Liang X, Hu Y, Wang Y, Yu H, Yang K. *p,p'*-DDE induces mitochondria-mediated
1001 apoptosis of cultured rat Sertoli cells. Toxicology 2008;253:53-61.
1002 Song Y, Shi Y, Yu H, Hu Y, Wang Y, Yang K. *p,p'*-Dichlorodiphenoxydichloroethylene induced
1003 apoptosis of Sertoli cells through oxidative stress-mediated p38 MAPK and
1004 mitochondrial pathway. Toxicol Lett 2011;202:55-60.
1005 Song Y, Wu N, Wang S, Gao M, Song P, Lou J, et al. Transgenerational impaired male fertility
1006 with an Igf2 epigenetic defect in the rat are induced by the endocrine disruptor *p,p'*-
1007 DDE. Hum Reprod 2014b;29:2512-21.
1008 Stemmler I, Lammel G. Cycling of DDT in the global environment 1950–2002: World ocean
1009 returns the pollutant. Geophys Res Lett 2009;36:L24602.
1010 Toft G. Persistent organochlorine pollutants and human reproductive health. Dan Med J 2014;
1011 61:B4967.
1012 Tranter R, Read JA, Jones R, Brady RL. Effector sites in the three-dimensional structure of
1013 mammalian sperm beta-acrosin. Structure 2000;8:1179-88.
1014 Valeron PF, Pestano JJ, Luzardo OP, Zumbado ML, Almeida M, Boada LD. Differential effects
1015 exerted on human mammary epithelial cells by environmentally relevant
1016 organochlorine pesticides either individually or in combination. Chem Biol Interact
1017 2009;180:485-91.
1018 van den Berg M, Kypke K, Kotz A, Tritscher A, Lee SY, Magulova K, et al. WHO/UNEP global
1019 surveys of PCDDs, PCDFs, PCBs and DDTs in human milk and benefit-risk evaluation of
1020 breastfeeding. Arch Toxicol 2017; 91: 83-96.
1021 Vieira CE, Costa PG, Lunardelli B, de Oliveira LF, Cabrera Lda C, Risso WE, et al. Multiple
1022 biomarker responses in *Prochilodus lineatus* subjected to short-term in situ exposure
1023 to streams from agricultural areas in Southern Brazil. Sci Total Environ 2016;542:44-56.

1024 Visconti PE, Westbrook VA, Chertihin O, Demarco I, Sleight S, Diekman AB. Novel signaling
1025 pathways involved in sperm acquisition of fertilizing capacity. J Reprod Immunol 2002;
1026 53:133-50.
1027 White FM. Quantitative phosphoproteomic analysis of signaling network dynamics. Curr Opin
1028 Biotechnol 2008;19:404-9.
1029 Winterbourn CC, Hampton MB. Thiol chemistry and specificity in redox signaling. Free Radic
1030 Biol Med 2008;45:549-61.
1031 Xu H, Kongmanas K, Kadunganattil S, Smith CE, Rupar T, Goto-Inoue N, et al. Arylsulfatase A
1032 deficiency causes seminolipid accumulation and a lysosomal storage disorder in Sertoli
1033 cells. J Lipid Res 2011;52:2187-97.
1034 Xu LC, Sun H, Chen JF, Bian Q, Song L, Wang XR. Androgen receptor activities of p,p'-DDE,
1035 fenvalerate and phoxim detected by androgen receptor reporter gene assay. Toxicol
1036 Lett 2006;160:151-7.
1037 Yan LJ, Forster MJ. Chemical probes for analysis of carbonylated proteins: a review. J
1038 Chromatogr B Analyt Technol Biomed Life Sci 2011;879:1308-15.
1039 Ying J, Clavreul N, Sethuraman M, Adachi T, Cohen RA. Thiol oxidation in signaling and
1040 response to stress: detection and quantification of physiological and
1041 pathophysiological thiol modifications. Free Radic Biol Med 2007;43:1099-108.
1042 Yoshitake H, Yanagida M, Maruyama M, Takamori K, Hasegawa A, Araki Y. Molecular
1043 characterization and expression of dipeptidase 3, a testis-specific membrane-bound
1044 dipeptidase: complex formation with TEX101, a germ-cell-specific antigen in the
1045 mouse testis. J Reprod Immunol 2011;90:202-13.
1046 Zhang K, Wei YL, Zeng EY. A review of environmental and human exposure to persistent
1047 organic pollutants in the Pearl River Delta, South China. Sci Total Environ 2013;463-
1048 464:1093-110.

1049 Zhao M, Shirley CR, Hayashi S, Marcon L, Mohapatra B, Suganuma R, et al. Transition nuclear
1050 proteins are required for normal chromatin condensation and functional sperm
1051 development. Genesis 2004;38:200-13.
1052 Zhou J, Sun Q, Yang Z, Zhang J. The hepatotoxicity and testicular toxicity induced by arecoline
1053 in mice and protective effects of vitamins C and E. Korean J Physiol Pharmacol 2014;
1054 18: 143-8.
1055

Table 1. List of proteins identified from peptides containing differentially oxidized Cys residues in mice testis after exposure to DDE.

Accession[a]	Protein name (Abbreviation)[a]	Peptide	Cys position	Cluster pattern[b]	Oxidized/Reduced Cys[c]			Biological function[d]
					Control	DDE10	DDE30	
P68254	14-3-3 protein theta (1433T)	YLAEVACGDDRK	134	D	0.11	0.22	0.20	
		YLAEVACGDDR	134	C	0.02	0.03	0.02	
P63101	14-3-3 protein zeta/delta (1433Z)	DICNDVLSLLEK	94	B	0.42	0.01	0.01	
P62858	40S ribosomal protein S28 (RS28)	TGSQGQCTQVR	27	C	0.04	0.06	0.03	
P35979	60S ribosomal protein L12 (RL12)	CTGGEVGATSALAPK	17	C	0.06	0.08	0.05	
P23578	Acrosin (ACRO)	IDTCQGDSGGPLMCR	247	A	36.36	64.52	208.33	1
		DNVDSPFVVVGITSWGVGCAR	269	B	28.90	20.45	18.48	
Q3V140	Acrosin-binding protein (ACRBP)	CSNHVYYAK	110	B	2.99	1.58	2.95	1
		CSQPVSILSPNTLK	122	D	37.59	103.09	68.03	
		LEQCHSEASVLR	382	B	13.91	0.12	0.15	
		ICDTNYIQYPNYCSFK	485	B	8.44	5.20	5.62	
P50289	Acrosomal protein SP-10 (ASPX)	GEGVCTTQNSQQCMLK	205,213	A	57.80	85.47	149.25	
		LQFMVQGCENMCPSMNLFSHGTR	231,235	C	33.44	71.94	24.88	
Q8CG76	Aflatoxin B1 aldehyde reductase member 2 (ARK72)	ACHQLHQEGK	164	C	0.06	0.10	0.05	2
P28474	Alcohol dehydrogenase class-3 (ADHX)	AGDTVIPLYIPQCGECK	97,100	B	0.76	0.55	0.61	2
		VCLLGCGISTGYGAAVNTAK	170	A	0.66	0.79	0.94	
		EFGASECISPQDFSK	240	B	0.42	0.24	0.21	
P29699	Alpha-2-HS-glycoprotein (FETUA)	ELACDDPEAEQVALLAVDYLNNHLLQGFK	32	D	1.37	15.24	7.18	
		ANLMHNLGGEEVSVACK	247	D	3.25	10.22	6.83	
Q9QWR8	Alpha-N-acetylgalactosaminidase (NAGAB)	MTCMGYPGTTLDK	127	D	0.77	3.95	2.78	
P09470	Angiotensin-converting enzyme (ACE)	EVVCHPSAWDFYNGK	962	C	13.05	14.90	5.41	1
P50428	Arylsulfatase A (ARSA)	AHFFTQGSAHSDTTSDPACHAANR	413	D	7.57	11.59	9.08	1
P28653	Biglycan (PGS1)	VGINDFCPMGFGVK	322	C	17.92	50.76	24.51	
P20060	Beta-hexosaminidase subunit beta (HEXb)	GIAAQPLYTGYCNYENK	530	B	42.37	40.00	23.87	1
Q60755	Calcitonin receptor (CALCR)	CYDRIHQLPSYEGEGLYCNR	72,89	C	12.41	41.32	14.37	
P14211	Calreticulin (CALR)	HEQNIDCGGGYVK	105	C	7.65	14.35	8.94	1, 3, 4
		DMHGDSEYNIMFGPDICGPGTK	137	D	15.06	28.17	22.57	
P18242	Cathepsin D (CATD)	GGCEAIVDTGTSLLVGPVEEVK	288	B	7.47	2.46	2.04	
Q09XV5	Chromodomain-helicase-DNA-binding protein 8 (CHD8)	QNCILADEMGLGK	834	B	20.00	19.19	12.74	

P70412	CUB and zona pellucida-like domain-containing protein 1 (CUZD1)	CTASLGGANLGETHK	32	D	0.37	1.45	1.83	1
		ILICDNNDQTSR	502	D	0.79	1.39	1.32	
Q9DAN8	Cystatin-12 (CST12)	YDEDIDNCPLQEGPGER	92	A	17.70	16.98	52.08	
P97315	Cysteine and glycine-rich protein 1 (CSRP1)	CSQAVYAAEK	122	B	0.55	0.39	0.24	
		GLESTTLADKDGEIYCK	167	A	0.15	0.13	0.16	
Q03401	Cysteine-rich secretory protein 1 (CRIS1)	YYYVCHYCPVGNYQGR	168,171	A	24.63	56.82	98.04	
		ATCLCEGK	237,239	A	6.63	11.20	41.67	
P99028	Cytochrome b-c1 complex sub. 6. mitochondrial (QCR6)	SQTEEDCTEELFDFLHAR	65	D	10.86	60.98	27.86	2
O08749	Dihydrolipoyl dehydrogenase. mitochondrial (DLDH)	NETLGGTCLNVGCIPSK	80,85	C	7.00	11.05	7.70	1, 2
		VLGAHILGPGAGEMVNEAALALEYGASCEDIAR	477	B	2.90	2.16	2.63	
		VCHAHPTLSEAFR	484	D	0.40	0.62	0.57	
Q9DA79	Dipeptidase 3 (DPEP3)	LRDGLVGAQFWSAYIPCQTQDR	143	B	0.21	0.18	0.09	1
Q99KV1	DnaJ homolog subfamily B member 11 (DJB11)	FQMTQEVVCDECPNVK	193,196	A	5.46	0.44	7.28	
Q9DC23	DnaJ homolog subfamily C member 10 (DJC10)	VDCQAYPQTCQK	728,735	A	10.88	9.29	16.78	2
Q9Z0J0	Epididymal secretory protein E1 (NPC2)	VPFPIPEPDGCK	93	D	15.48	38.31	27.86	
A2AJB7	Epididymal-specific lipocalin-5 (LCN5)	HDLTCVNALQSGQI	183	B	5.21	3.10	3.10	
O08716	Fatty acid-binding protein 9 (FABP9)	VACLIKPSVSISFNGER	35	B	3.69	3.27	3.29	
		MDIQAGSACR	58	C	5.38	11.34	5.92	
P09528	Ferritin heavy chain (FRIH)	LATDKNDPHLCDFIETYYLSEQVK	131	D	1.62	2.75	2.80	2
Q9QXC1	Fetuin-B (FETUB)	THTTCPDCPSPIDLSNPSALEAATESLAK	154,157	A	8.90	10.03	14.49	1
Q8VCM7	Fibrinogen gamma chain (FIBG)	VAQLEAQCQEPCK	160	D	0.40	0.73	0.60	3
O08795	Glucosidase 2 subunit beta (GLU2b)	YEQGTGCWQGPNR	464	C	16.08	59.17	21.05	
O35660	Glutathione S-transferase Mu 6 (GSTM6)	HNLCGETEEER	87	C	0.01	0.02	0.01	2
Q80W21	Glutathione S-transferase Mu 7 (GSTM7)	LCYNADFEK	115	C	0.05	0.08	0.04	2
Q9CPV4	Glyoxalase domain-containing protein 4 (GLOD4)	HEEFEEGCK	41	A	11.70	13.21	19.76	
		AACNGPYDGK	45	B	7.78	1.82	7.12	
P63017	Heat shock cognate 71 kDa protein (HSP7c)	CNEIISWLDK	574	C	0.03	0.07	0.02	4
P16627	Heat shock 70 kDa protein 1-like (HS71l)	LYQSGCTGPTCTPGYTPGR	617,622	B	5.84	5.17	3.28	1, 4
P07901	Heat shock protein HSP 90-alpha (HS90a)	KCLELFTELAEDKENYK	421	B	1.10	0.41	1.06	4
		CLELFTELAEDKENYK	421	A	0.99	0.38	6.74	
Q91X72	Hemopexin (HEMO)	GECQSEGVLFFQGNR	153	C	7.59	8.95	6.97	
		DYFVSCPGR	230	B	106.38	35.71	26.60	
Q8BG05	Heterogeneous nuclear ribonucleoprotein A3 (ROA3)	WGTLTDCVVMR	64	C	0.01	0.03	0.01	
Q9Z2X1	Heterogeneous nuclear ribonucleoprotein F (HNRPF)	DLSYCLSGMYDHR	267	C	0.15	0.25	0.12	

P61979	Heterogeneous nuclear ribonucleoprotein K (HNRPK)	GSDFDCELR	145	C	0.02	0.02	0.01	
Q6S9I3	HMW kininogen-II	ESNTELTEDCEIK	339	D	24.04	55.56	38.02	3
Q9D5A9	Inactive ribonuclease-like protein 10 (RNS10)	IKEPNQSCINQYTFIHEDPNTVK	128	C	2.64	5.18	0.61	1
Q05CL8	La-related protein 7 (LARP7)	ESAVDSSSSGVCK	243	B	11.44	0.31	0.26	1
Q8BVP2	L-lactate dehydrogenase (LDH)	IIGSGCNLDTAR	213	C	0.05	0.09	0.04	2
P11438	Lysosome-associated membrane glycoprotein 1 (LAMP1)	CNTEEHIFVSK	327	A	6.91	5.19	15.31	1
Q61830	Macrophage mannose receptor 1 (MRC1)	TGVAGGLWDVLSCEEK	617	B	22.22	13.28	8.21	
E9Q5I3	Mucin 5, subtype B, tracheobronchial	IVTENVPCGTTGTTCSK	949,956	A	9.07	17.39	29.67	
		CMAQNYPGVNVDK	1911	A	2.56	3.80	7.46	
P11378	Nuclear transition protein 2 (STP2)	SCSQAGHAGSSSSPSPGPPMK	41	C	0.58	0.82	0.46	1
P35700	Peroxiredoxin-1 (PRDX1)	HGEVCPAGWKPGSDTIKPDVNK	173	C	0.99	1.09	0.70	2
P99029	Peroxiredoxin-5 mitochondrial (PRDX5)	GVLFGVPGAFTPGCSK	96	B	1.81	1.28	0.99	2
P45878	Peptidyl-prolyl cis-trans isomerase (FKBP2)	GWDQGLLGMCEGEK	95	D	2.84	5.64	4.16	4
O70250	Phosphoglycerate mutase 2 (PGAM2)	FCGWFDAELSEK	23	C	0.09	0.11	0.06	1
P20918	Plasminogen (PLMN)	TPENFPDAGLEMNYCR	426	B	13.68	3.72	3.08	3
Q8CFJ5	Predicted gene 4763	CYFSDMTVEGGGLK	113	C	22.88	30.12	13.70	
Q921X9	Protein disulfide-isomerase A5 (PDIA5)	DKNQDLCQQEAVK	463	C	0.63	0.71	0.46	2
Q91VU0	Protein FAM3C	ICLEDNVLMSGVK	86	A	0.10	0.03	0.33	
Q3TCN2	Putative phospholipase B-like 2 (PLPL2)	YNDFLHDPLSLCEACNPKPNAENAISAR	497,500	A	3.59	4.72	15.67	
P56959	RNA-binding protein (FUS)	CPNPTCENMNFSWR	421,426	D	0.03	0.04	0.05	1
Q8CEK3	Serine protease inhibitor kazal-like protein, minor form (SPIKL)	SECSNIAENPVCADDR	48,57	B	227.27	42.37	43.86	1
Q8BMY7	Serine protease inhibitor Kazal-type 2 (ISK2)	TPDCGHFDFPACPR	38,46	B	12.11	8.46	1.97	1
P07724	Serum albumin (ALBU)	YMCENQATISSK	289	D	10.10	16.67	15.38	
		LQTCCDKPLLK	302,303	D	22.27	26.39	25.25	
		LPCVEDYLSAILNR	472	C	0.40	1.34	0.48	
		AETFTFHSDICTLPEK	538	A	0.01	0.00	0.02	
		AADKDTCFSTEGPNLVTR	591	A	2.52	1.54	2.87	
Q921I1	Serotransferrin (TRFE)	WCAVSEHENTK	28	D	3.37	10.38	11.64	
		AVSSFFSGSCVPCADPVAFPK	177,180	A	10.36	4.51	25.32	
		NQQEGVCPEGSIDNSPVK	350	A	0.21	5.58	13.62	
		TKCDEWSIISEGK	373	A	8.34	8.87	13.55	
		FDEFFSQGCAPGYEK	506	D	3.38	22.68	31.35	
		QEDFELLCPDGTR	583	C	500.00	625.00	285.71	
		LLEACTFHK	692	A	3.94	5.79	7.69	

Q9DA48	Sperm acrosome membrane-associated protein 1 (SACA1)	EVILTNGCPGGESK	111	A	0.03	0.04	0.14	1
		GPVDCGWGKPISENLDSAR	131	B	12.94	8.89	1.51	
		LSCVHISPENR	148	D	2.33	5.29	6.49	
Q9D9X8	Sperm acrosome membrane-associated protein 3 (SACA3)	TLASNGPNLCR	168	C	8.23	40.16	6.05	1
P70302	Stromal interaction molecule 1 (STIM1)	NTGASSGATSEESTEAEFCR	49	C	21.19	91.74	16.61	
Q8CH09	SURP and G-patch domain-containing protein 2 (SUGP2)	EDQASTPGLSQASSGSCFPR	932	C	0.74	1.33	0.75	
Q9JMI7	Testis-expressed protein 101 (TEX101)	AEQCNPGELCQETVLLIK	53,59	B	30.30	10.40	25.77	1
		GCTTTIGCR	186	A	105.26	40.00	117.65	
		ETCSYQSFLQPR	210	A	24.21	21.93	26.11	
P10639	Thioredoxin (THIO)	LVVVDFSATWCGPCK	32,35	A	25.45	8.52	52.91	2
Q91W90	Thioredoxin domain-containing protein 5 (TXND5)	VDCTADSDVCSAQGVR	107,114	C	40.00	90.91	38.46	2
Q01853	Transitional endoplasmic reticulum ATPase (TERA)	AIANECQANFISIK	535	C	0.01	0.04	0.01	
Q9R0P9	Ubiquitin carboxyl-terminal hydrolase isozyme L1 (UCHL1)	NEAIQAAHDSVAQEGQCR	162	D	0.03	0.05	0.04	
A2AFS3	UPF0577 protein KIAA1324	ESEYHFEYTACDSTGSR	61	D	0.00	18.28	24.21	

[a] Protein name, abbreviation and accession obtained from UniProtKB/Swiss-Prot database.

[b] Cluster patterns of peptides as in Fig. 4.

[c] The redox state of selected redox Cys residues labeled with both d(0) NEM and d(5) NEM was calculated using the ratio of the average ion intensity of parents ions. The m/z values and retention times of selected peptides were applied in the targeted approach using Skyline open software.

[d] Terms defining the main biological functions of the identified proteins are indicated as follows: 1, related with reproduction; 2, connected to oxidative stress; 3, negative regulation of blood coagulation, or 4, involved in protein folding.

Figure 1

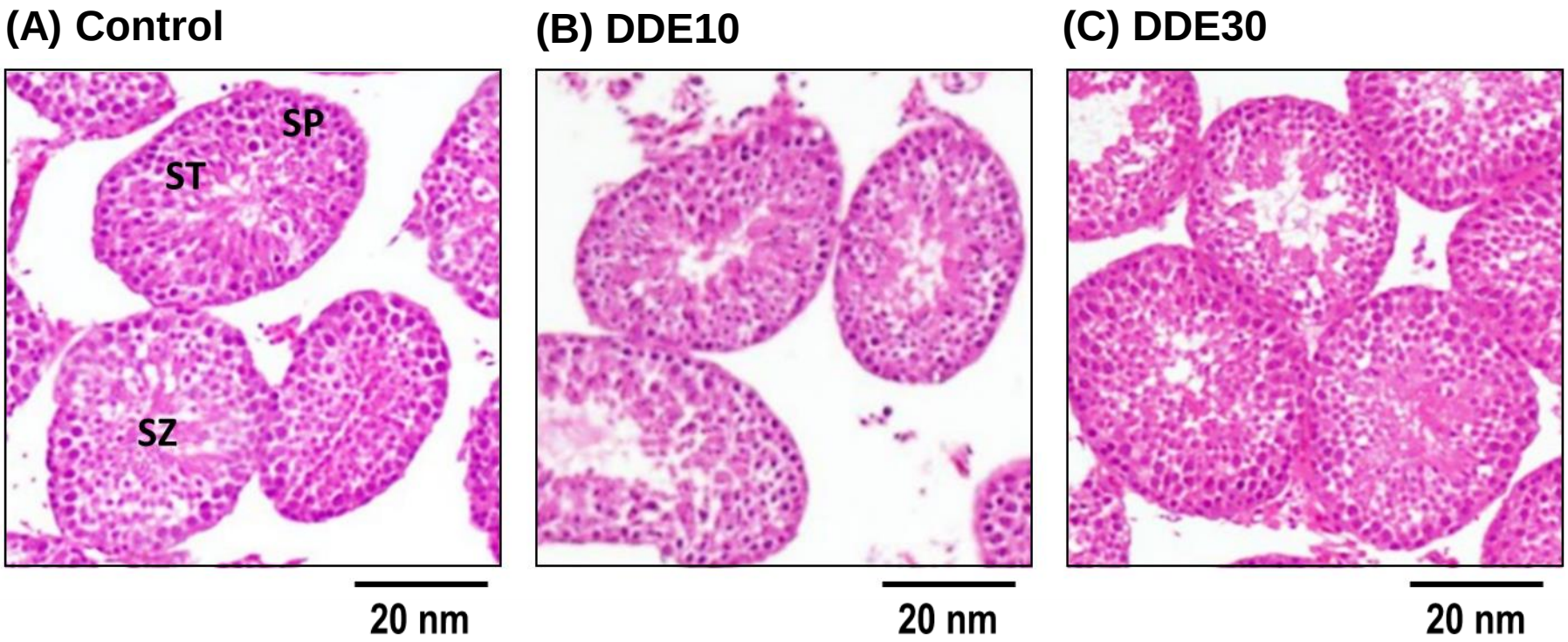

Figure 2

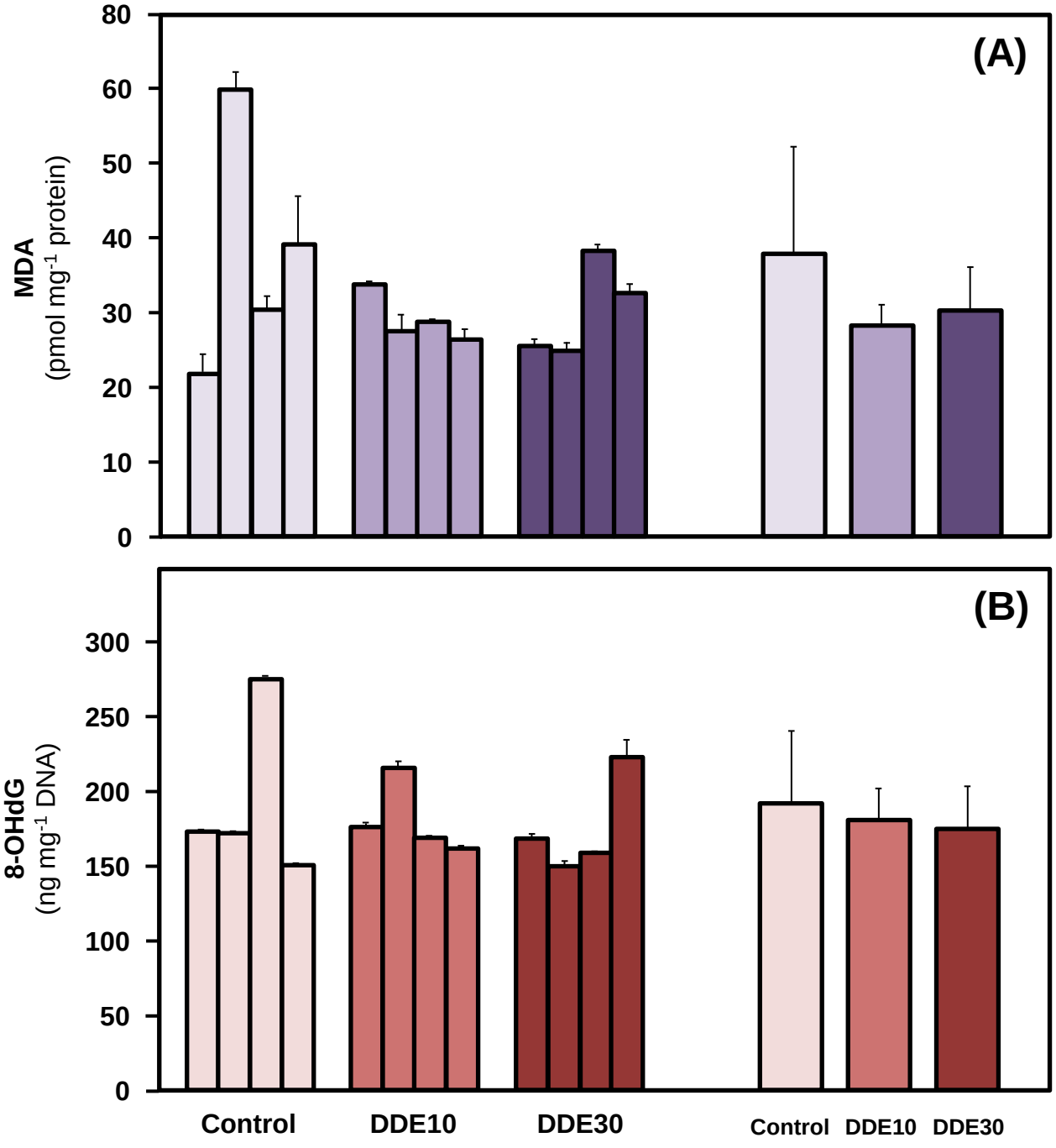
(A)
MDA
(pmol mg-1 protein)
80
60
50
40
30
20
10
0
(B)
8-OHdG
(ng mg-1 DNA)
300
250
200
150
100
50
0
Control
DDE10
DDE30
Control
DDE10
DDE30

Figure 3

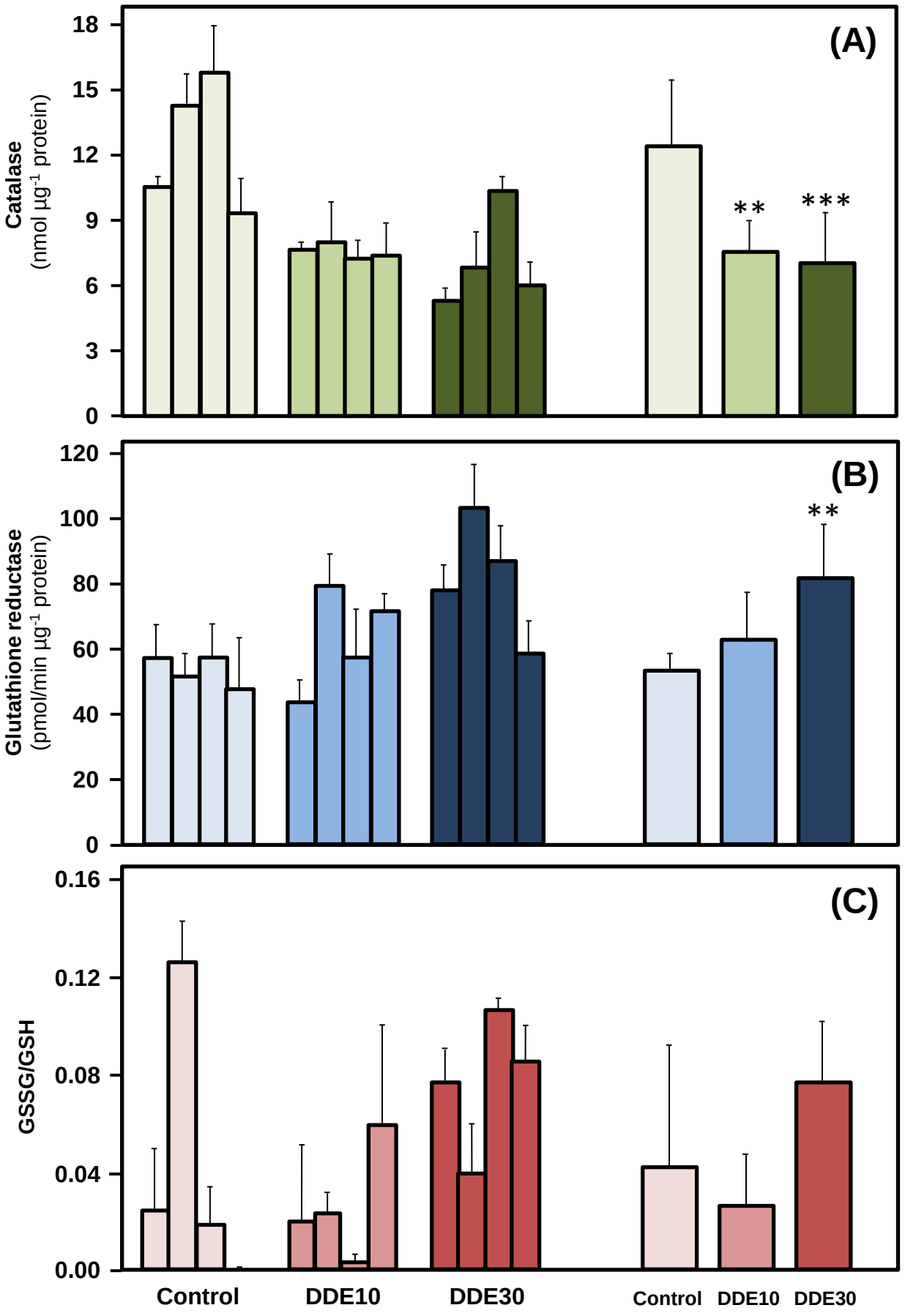
(A)
Catalase
(nmol µg-1 protein)
18
15
12
9
6
3
0
**
***
(B)
Glutathione reductase
(pmol/min µg-1 protein)
120
100
80
60
40
20
0
**
(C)
GSSG/GSH
0.16
0.12
0.08
0.04
0.00
Control
DDE10
DDE30
Control
DDE10
DDE30

Figure 4

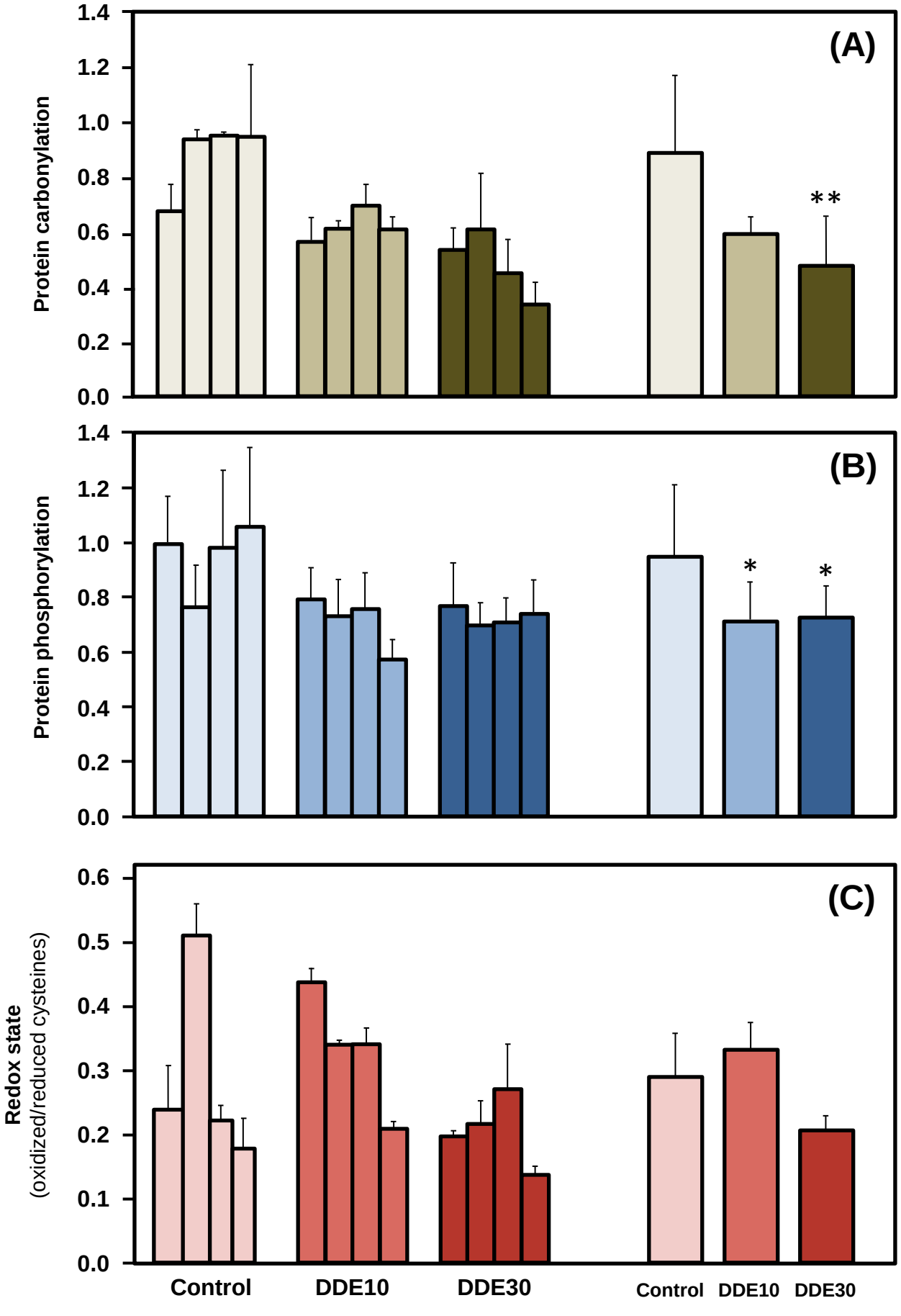
(A)
Protein carbonylation
1.4
1.2
1.0
0.8
0.6
0.4
0.2
0.0
**
(B)
Protein phosphorylation
1.4
1.2
1.0
0.8
0.6
0.4
0.2
0.0
*
*
(C)
Redox state
(oxidized/reduced cysteines)
0.6
0.5
0.4
0.3
0.2
0.1
0.0
Control
DDE10
DDE30
Control
DDE10
DDE30

Figure 5

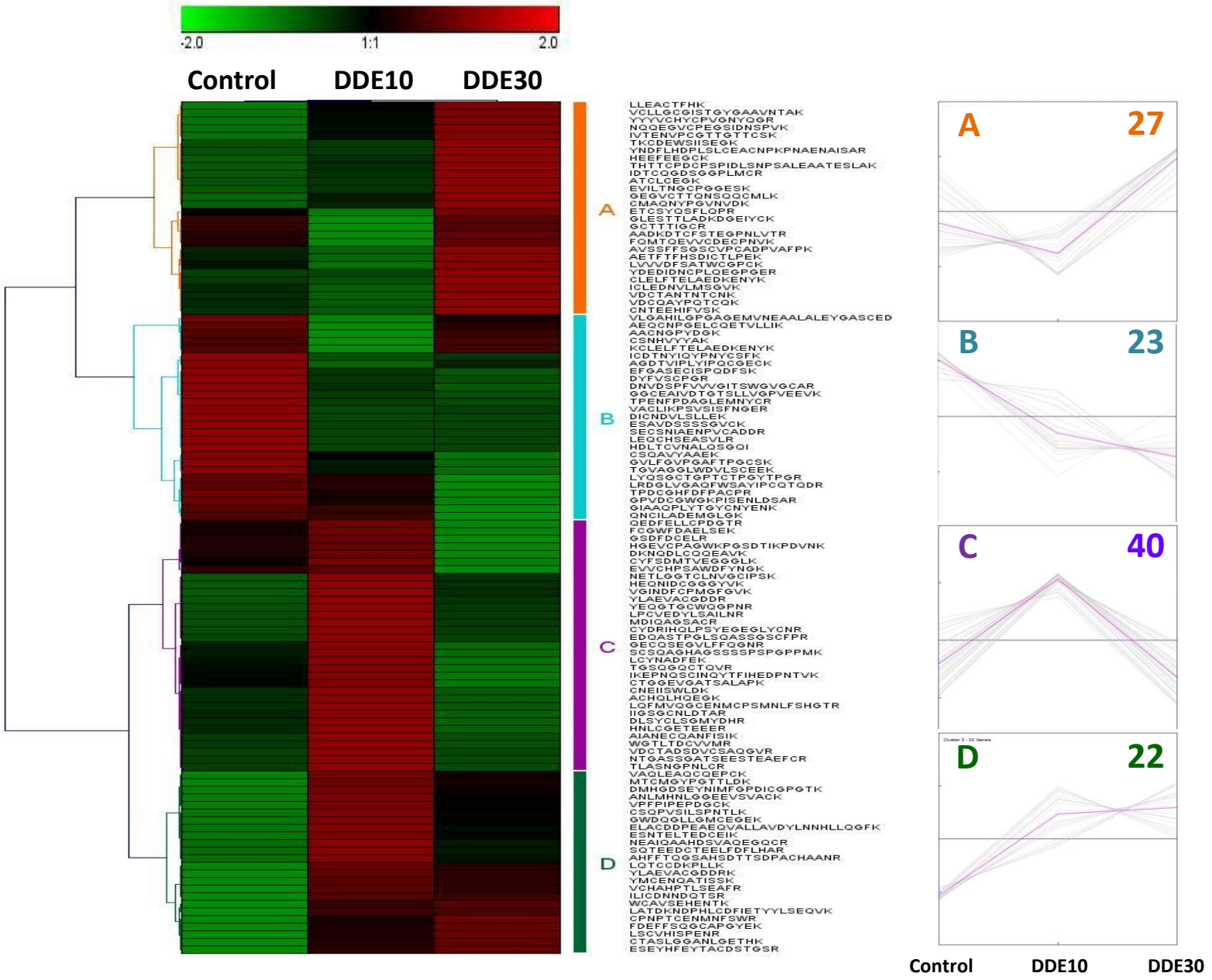
-2.0
1:1
2.0
Control
DDE10
DDE30
A
B
C
D
A 27
B 23
C 40
D 22
Control
DDE10
DDE30

Figure 6

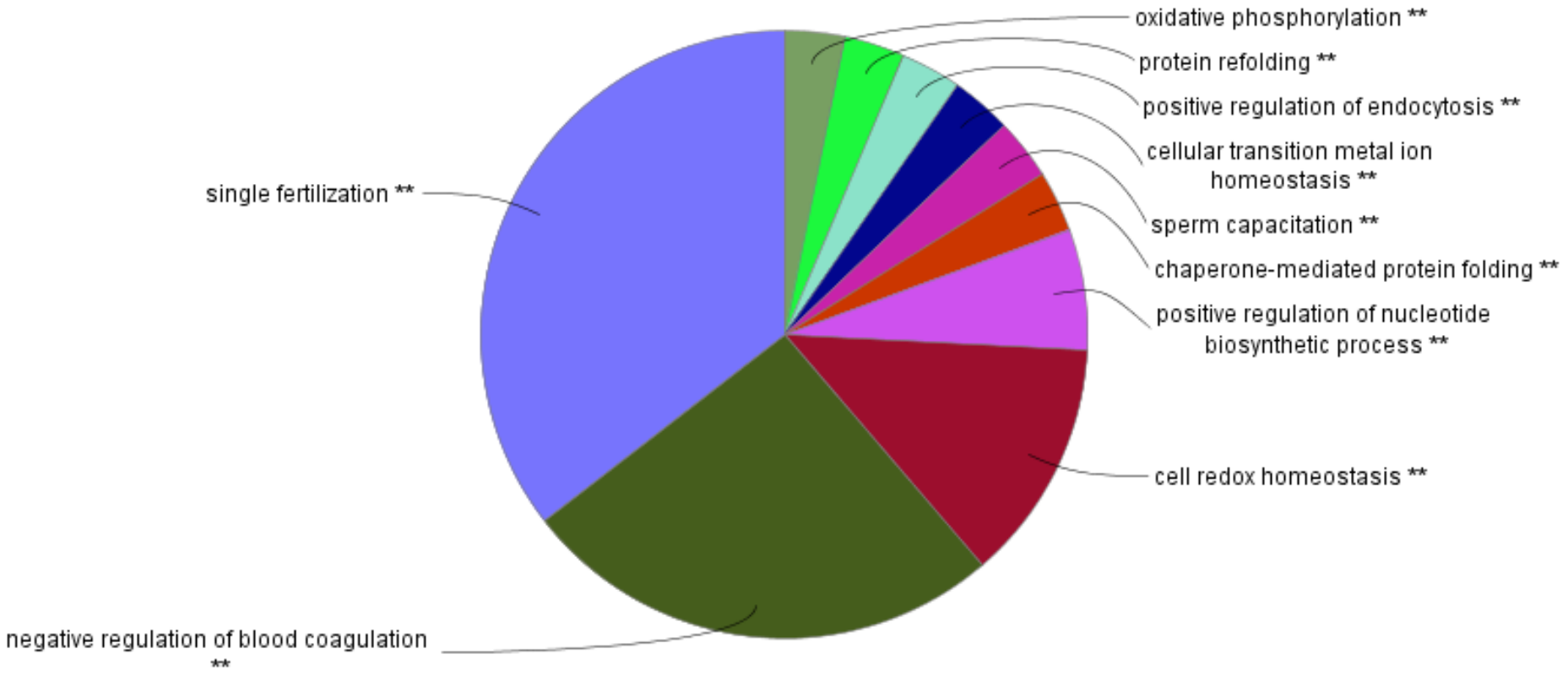
oxidative phosphorylation **
protein refolding **
positive regulation of endocytosis **
cellular transition metal ion homeostasis **
sperm capacitation **
chaperone-mediated protein folding **
positive regulation of nucleotide biosynthetic process **
cell redox homeostasis **
negative regulation of blood coagulation **
single fertilization **